Plant Biotechnology Journal
Open Access

*Plant Biotechnology Journal* (2020) **18**, pp. 2328–2344 doi: 10.1111/pbi.13394

# Loss of function of CRT1a (calreticulin) reduces plant susceptibility to *Verticillium longisporum* in both *Arabidopsis thaliana* and oilseed rape (*Brassica napus*)

Michael Pröbsting[1,†], Dirk Schenke[1,*,†], Roxana Hossain[2,†], Claudia Häder[1], Tim Thurau[1], Lisa Wighardt[1], Andrea Schuster[1], Zheng Zhou[1], Wanzhi Ye[1], Steffen Rietz[3], Gunhild Leckband[3] and Daguang Cai[1,*]

[1]*Department of Molecular Phytopathology and Biotechnology, Institute of Phytopathology, Christian-Albrechts-University of Kiel, Kiel, Germany*
[2]*Institut für Zuckerrübenforschung, Göttingen, Germany*
[3]*Hohenlieth-Hof, NPZ Innovation GmbH, Holtsee, Germany*

*Received 10 February 2020;*
*revised 6 April 2020;*
*accepted 11 April 2020.*
**Correspondence* (Tel +49-431-8803215; fax +49-431-8801583; email dcai@phytomed.uni-kiel.de (DC); Tel +49-431-8804887; fax +49-431-8801583; email d.schenke@phytomed.uni-kiel.de (DS))
[*]These authors contributed equally.

**Keywords:** CRT1a, calreticulin, CRISPR/Cas9, TILLING, recessive resistance, susceptibility factor, *Verticillium longisporum*, *Brassica napus*, *Arabidopsis thaliana*.

## Summary

*Brassica napus* is highly susceptible towards *Verticillium longisporum* (*Vl43*) with no effective genetic resistance. It is believed that the fungus reprogrammes plant physiological processes by up-regulation of so-called susceptibility factors to establish a compatible interaction. By transcriptome analysis, we identified genes, which were activated/up-regulated in rapeseed after *Vl43* infection. To test whether one of these genes is functionally involved in the infection process and loss of function would lead to decreased susceptibility, we firstly challenged KO lines of corresponding Arabidopsis orthologs with *Vl43* and compared them with wild-type plants. Here, we report that the KO of *AtCRT1a* results in drastically reduced susceptibility of plants to *Vl43*. To prove *crt1a* mutation also decreases susceptibility in *B. napus*, we identified 10 mutations in a TILLING population. Three T3 mutants displayed increased resistance as compared to the wild type. To validate the results, we generated CRISPR/Cas-induced *BnCRT1a* mutants, challenged T2 plants with *Vl43* and observed an overall reduced susceptibility in 3 out of 4 independent lines. Genotyping by allele-specific sequencing suggests a major effect of mutations in the *CRT1a* A-genome copy, while the C-genome copy appears to have no significant impact on plant susceptibility when challenged with *Vl43*. As revealed by transcript analysis, the loss of function of *CRT1a* results in activation of the ethylene signalling pathway, which may contribute to reduced susceptibility. Furthermore, this study demonstrates a novel strategy with great potential to improve plant disease resistance.

## Introduction

*Brassica napus* or commonly referred to as oilseed rape (OSR) is a commercially important crop and grown to produce vegetable oil for human consumption, animal feeding and biodiesel utilization (Harloff *et al.*, 2012). In 2018, OSR was after soya bean the second most cultivated oilseed crop with 70.91 million tons, worldwide (USDA, 2018). The advantage of OSR is the viability at low temperatures with reasonable humidity; thus, it can be cultivated in temperate zones where soya bean and sunflower are not able to be cultivated. Since the 1970s, the worldwide cultivation area has increased continuously (FAOSTAT, 2016). A consequence of the increased production area in addition to narrow crop rotation cycles and tillage operations is the enrichment of soilborne pathogens, such as *Verticillium longisporum* (De Coninck *et al.*, 2015).

*Verticillium longisporum* is a hemibiotrophic fungal pathogen specialized to infect Brassicaceae and causes Verticillium stem striping in OSR (Depotter *et al.*, 2016). It emerges especially in northern Europe and attacks preferentially developing plant roots (Johansson *et al.*, 2006). The infection process starts with the germination of fungal microsclerotia that recognize root exudates and follow the nutrient gradient to reach the roots of potential host plants. The fungus can directly penetrate the epidermal cells of the root and, in addition, natural openings, for example wounds are used by the fungus to infect the host, spreading inter- and intracellularly, finally resulting in hyphal proliferation and the production of conidia (Depotter *et al.*, 2016; Johansson *et al.*, 2006). The fungus accomplishes extensive colonization of the whole plant by using the vascular system to spread its conidia. During later stages of plant colonization, the fungus resigns from the vascular elements and starts a necrotrophic life phase by feeding on senescing leaf and stem tissue (Reusche *et al.*, 2012).

Oilseed rape is an amphidiploid species (2n = 38, AACC genome) derived from the hybridization of the two closely related species *Brassica rapa* (AA) and *Brassica oleracea* (CC) (Nagaharu, 1935). The relatively young age of this species goes along with a very limited genetic pool, which was further narrowed because the breeding focus was on double zero lines. Several problems such as inferior seed germination (Hatzig *et al.*, 2018) or reduced pathogen resistance (Zhao and Meng, 2003) arose from these breeding strategies. For instance, genetic resources for resistance breeding to control Verticillium stem striping in OSR are hardly available, and so far, no effective resistance has been described. In practice, reducing the potential infection rate through minimizing the spore density in the soil is

often a main countermeasure, but very laborious or detrimental to non-target organisms under field conditions (Depotter *et al.*, 2016). In addition, no fungicide treatments are available to control this soilborne disease, and due to the colonization of the host through the vascular system, a contact fungicide treatment is anyway impossible. Thus, breeding for OSR resistance to fungal diseases is also the most favoured countermeasure against *V. longisporum* (Dunker *et al.*, 2008).

Worldwide, efforts have been made to identify genetic resistance resources by screening-related wild species (Eynck *et al.*, 2009; Happstadius *et al.*, 2003) including the parental species *B. oleracea* and *B. rapa* and generated resynthesized lineages (Eynck *et al.*, 2009). However, the resistance identified so far is highly polygenic (Eynck *et al.*, 2009; Rygulla *et al.*, 2008) and hardly suitable for breeding programmes. Thus, an alternative solution is needed. Increasing data demonstrates that a successful fungal colonization often relies on intensive plant–fungus interactions, involving negative defence regulators and susceptibility/compatibility factors (Behrens *et al.*, 2019). The loss of such factors in plants can cause an incompatible plant–pathogen interaction, thus providing a promising alternative for resistance breeding (Langner *et al.*, 2018). This approach was successfully applied to increase plant resistance to viral, bacterial, and fungal infections. For example, mutation of the eukaryotic translation initiation factor 4 (eIF4E/G) leads to virus resistance in a wide variety of plant species including barley, cucumber and rice (Chandrasekaran *et al.*, 2016; Macovei *et al.*, 2018; Stein *et al.*, 2005), and increased resistance towards the bacterial pathogen *Xanthomonas* was reported by mutation of SWEET sucrose transporters in rice, cassava or citrus, respectively (Oliva *et al.*, 2019; Zhou *et al.*, 2015; Cohn et al., 2014; Hu *et al.*, 2014). Furthermore, as demonstrated in barley, a nucleotide mutation in *Mlo* confers a durable resistance to powdery mildew since several years (Kusch and Panstruga, 2017). Loss of function in all *Mlo* alleles also generated powdery mildew resistance in grape, tomato and wheat (Malnoy *et al.*, 2016; Nekrasov *et al.*, 2017; Wang *et al.*, 2014).

It is extremely difficult to identify natural loss-of-function mutations in crops with complex genomes due to functional redundancy caused by many alleles encoding the same gene. Recently, methods have been successfully developed to increase genetic variation by mutating the whole crop genome, for example using the chemical ethyl methanesulphonate (EMS). The laborious identification of such EMS-caused point mutations can be achieved by Targeting Induced Local Lesions IN Genomes (TILLING; McCallum *et al.*, 2000; Till *et al.*, 2006). These mutations have to be combined by crossing, and phenotyping can be impeded by the many unwanted background mutations arising from this untargeted approach. Though it was actually possible to combine TILLING mutations for all six wheat *Mlo* alleles to generate a complete KO and therefore to increase resistance to powdery mildew (Acevedo-Garcia *et al.*, 2017), a study by Wang *et al.* (2014) appeared three years earlier using a targeted genome editing approach involving side-specific nucleases (SSN).

The allotetraploid genome of *Brassica napus* is also very complex (Chalhoub *et al.*, 2014). SSNs such as CRISPR/Cas have recently been successfully deployed to induce mutations in OSR to improve agronomic traits such as silique development and seed shatter resistance (Braatz *et al.*, 2017; Yang *et al.*, 2017; Yang *et al.*, 2018; Zhai *et al.*, 2019a), branching (Zheng *et al.*, 2019), increase in the content of oleic acid (Okuzaki *et al.*, 2018), altered oil content and fatty acid composition in seeds (Zhai *et al.*, 2019b) or resistance to *Sclerotinia sclerotiorum* by WRKY70 KO (Sun *et al.*, 2018). Thus, SSNs can efficiently mutate a target gene in less time compared to TILLING and reduce unwanted off-target mutations in OSR.

The aim of this work was to increase the resistance of OSR towards *V. longisporum* infection by interrupting the compatible plant–fungus interaction *via* mutation of candidate host susceptibility genes identified by functional genomics. Twenty candidate genes with altered expression levels in response to infection with *V. longisporum* isolate 43 (*Vl43*) were identified from two suppression subtractive hybridization (SSH) libraries (Diatchenko *et al.*, 1996). Here, we report that loss of function of CRT1a (calreticulin) strongly reduces plant susceptibility to *V. longisporum* in both *A. thaliana* and OSR, demonstrating thereby a strategy and working routine allowing for an efficient generation of recessive resistance against pathogens in OSR.

## Results

### Identification of CRT1a as putative susceptibility factor

In order to identify genes being substantially involved in the *Brassica napus–Vl43* interaction, we constructed two SSH libraries. *Brassica napus* Express 617 plants were infected with *Vl43,* and mRNA was isolated at 5, 10 and 15 days postinoculation (dpi). The pooled mRNAs from infected and mock samples were used to produce the SSH libraries. For the 'forward' library, we used mRNA from infected material as tester and control mRNA as driver to identify up-regulated genes and *vice versa* in the 'reverse' library to identify down-regulated genes. In total, we obtained 1060 sequences from the forward library of which 907 were plant-derived, representing 413 unique plant genes. 461 sequences were obtained from the reverse library with 369 being plant-derived, representing 209 unique plant genes. The complete list of sequenced clones with homologies to plant genes is presented in Table S1. Potential susceptibility factors are expected to be up-regulated by the pathogen to achieve colonization of its host; thus, our main interest lies on the forward library. However, it is well known that during pathogen infection genes of the plant resistance response might be also suppressed, either by the pathogen or by the host, involving, for example, negative regulators of the innate immunity. Thus, a subset of candidates from the reverse library was also selected. In order to verify the quality of the SSH libraries, we checked the expression levels of randomly selected genes by RT-qPCR, which generally confirmed up- and down-regulation of genes obtained from the forward and reverse libraries, respectively (Figure S1). The selection of candidate genes for further analysis was based on inclusion of a wide range of differentially regulated genes and genes functionally related to plant–pathogen interactions, as well as genes with so far no connection to pathogenesis to identify novel components. A GENEVESTIGATOR-based meta-analysis (Hruz *et al.*, 2008) demonstrates a high functional divergence of 20 selected candidate genes (Tables S2 and S3). Since a knockout of these genes in the complex *Brassica napus* genome is still technically challenging and time-consuming, we employed firstly T-DNA insertion mutants of the corresponding Arabidopsis orthologs to investigate their functional involvement in the plant–*Vl43* interaction.

For 15 of the 20 candidate genes, we obtained homozygous Arabidopsis mutants (Table S3). We challenged these mutants with *Vl43* and compared the results with Col-0 wild-type plants with respect to disease progression and symptom development.

 

Strikingly, as most of the Arabidopsis mutants did not show obvious effects interfering with *Vl43,* the *crt1a* knockout led to significantly reduced susceptibility and symptom development (Figure 1). While at 28 dpi, the wild-type plants severely suffered from the infection and displayed the stunted shoot growth and senescence-like symptoms, the crt1a mutant was less affected by *Vl43* infection (Figure 1A). In accordance, the rosette diameter and the leaf area were less reduced (Figure 1B) and the fungal colonization/biomass was drastically decreased in the crt1a mutant plants as compared to the wild type (Figure 1C). In a time course experiment, we challenged the *crt1a* mutant and the Col-0 plants with varying conidia concentrations as high as up to $1 \times 10^7$ $mL^{-1}$. Again, we observed that the wild-type Col-0 plants severely suffered from the fungal infection, while the *crt1a* mutant plants survived and displayed impaired disease development (Figure S2). Taken together, these data strongly suggest that the knockout/loss of function of CRT1a reduces susceptibility of plants to *Vl43* infection. In the next step, we analysed the expression of CRT1a in response to *Vl43* infection by RT-qPCR in both Arabidopsis and OSR and found expression of calreticulin was significantly up-regulated in both species at 6 dpi (Figure 1D), in consistence with its identification from the SSH forward library.

In Arabidopsis, calreticulin (CRT) has three paralogs (CRT1a, CRT1b and CRT3), being an ER-localized protein with three major domains (Figure 1E). Calreticulins function in protein folding and $Ca^{2+}$ homeostasis (TAIR; Berardini *et al.*, 2015). When searching for the corresponding *Brassica napus* orthologous copies in the GENOSCOPE database (Chalhoub *et al.*, 2014), four sequences with high homology on cDNA and amino acid level were identified (Figure 1F). However, the sequences of BnaA09g15970 and BnaC01g43040 contained duplicated regions, probably due to wrong NGS annotation (Figure S3A). After removal of these duplicated regions, both sequences resemble very well CRT1a and all loci appear to be expressed (Figure S3B). Thus, we believe there are four functional *CRT1a* loci within the *Brassica napus* genome. In addition, a GENEVESTIGATOR meta-analysis revealed that Arabidopsis *CRT1a* is up-regulated in response to several other pathogens, such as *Blumeria graminis*, *Golovinomyces orontii*, *Phytophthora infestans*, *Sclerotinia sclerotiorum* and *Xanthomonas campestris,* and the PAMP elf18 and salicylic acid (Table S2). Furthermore, the impact of the AtCRT1a KO on agronomic traits, such as flowering time, plant height and number of siliques, was determined (Table S4). Collectively, the data suggest that CRT1a loss of function reduced the susceptibility of Arabidopsis to *Vl43* without negatively affecting the agronomic traits analysed. Thus, this gene was chosen for further investigation in *Brassica napus*.

## TILLING of CRT1a in *Brassica napus*

To generate allele-specific primer for TILLING at the CRT1a locus, we did bioinformatic analysis of the 4 CRT1a loci in the *Brassica napus* genome (Figures S3 and S4). From these, the CRT1a locus BnaA09g15970D is matching 100% to the EST 6F11-F8 from the SSH library; thus, we focused on identification of TILLING mutations in this gene, which we believe is the 'active' locus (Figures 6A and S4). We developed allele-specific primers for BnaA09g15970D covering the CRT1a genomic region containing exons 4–9 (Table S5; Figure 2A) and used them for TILLING at the CRT1a locus of an EMS-mutagenized OSR population established at the CAU (Harloff *et al.*, 2012). This TILLING fragment of 1082 bps represents 41.7% of the genomic region (Figure 2B). Screening of 3840 individual plants resulted in 131 potential mutation signals. With the aid of a specific pooling strategy (Harloff *et al.*, 2012), 64 signals could be attributed to single plants (Table S5). Due to degradation of some storage plant DNAs and failure of PCRs, only 27 single plants were available and subsequently subjected to sequencing in order to validate the mutations (Table S5). In total, 16 of 27 sequenced candidates showed an expected single nucleotide mutation triggered by EMS. Considering only mutations in the exonic region leading to an alternation in the amino acid sequence (mis-sense mutation), we focused on five cases with a nucleotide transition from G to A and on four cases with a C-to-T transition or SNP. Three of these mutants showed a change from tryptophan to a pre-mature stop codon, thus leading to a potential knockout of *CRT1a* (Figure 2C).

To investigate possible effects of these changes on OSR in regard to *Vl43* infection, we challenged the mutant plants with *Vl43* under greenhouse conditions in two independent experiments in which the susceptible line Express 617, the donor of the EMS population, and a resistant breeding line of NPZ served as controls. The plant growth and the development of disease symptoms were photographically documented weekly. As shown in Figure 2D, typical disease symptoms such as yellowing of leaves, necrosis and dieback of plants appeared as expected in the control plants, while the OSR mutants showed varied responses to the *V. longisporum* infection.

A disease rating was conducted at 35 dpi (Zeise and von Tiedemann, 2002) showing the resistant line has a constant rating of about 3 similar to non-infected plants, while the susceptible control Express 617 exhibited the typical disease symptoms capable of ratings up to 9 for dead plants. Plants from mutants 1510_4, 1819_4 and 1898_1 showed comparable disease symptoms to Express 617. Mutant 1047_2, from which all plants died at 35 dpi, appeared to be hyper-susceptible to *Vl43* infection. Mutant 1484_3 showed a similar rating as Express 617. Nevertheless, one plant from 1484_3 and two plants from 1752_4 could be scored 3 for resistance. However, seven individual plants from mutants 1873_3 and 1873_4 were scored similar to non-infected control plants (Figure 2E).

In addition, stunting symptoms were measured at 35 dpi. As shown in Figure 3A, the susceptible control Express 617 displays clear reduction in plant height to 60.5% of non-infected control plants. The hyper-susceptible mutant 1047_2 showed 100% stunting since all plants were dead. Mutants 1898_1, 1819_4 and 1752_4 revealed a comparable stunting as observed for Express 617 (60.5%), while the mutants 1484_3 and 1510_4 displayed a slightly reduced stunting effect. The knockout mutant 1873_4 showed a reduced stunting degree of only 37.2% compared to non-infected control plants and the mutant 1873_3 even less stunting (17.9%). These data suggest that the OSR *crta1a* mutants 1873_3 and 1873_4 represent the most promising mutant plants with decreased susceptibility to *V. longisporum* infection. In support for this, the fungal biomass, quantified by qPCR in root material of mutants 1873_3 and 1873_4, was much less than in the susceptible control Express 617 (Figure 3B), suggesting an impeded infection process of *Vl43* in both mutants. When comparing the disease phenotype of control and infected WT and mutant (1873_4) plants, we observed no growth reduction by infection in the mutant (Figure 3C).

Unexpectedly, mutant 1047_2 also carrying a stop codon in BnaA09g15400D was rather hyper-susceptible and not able to

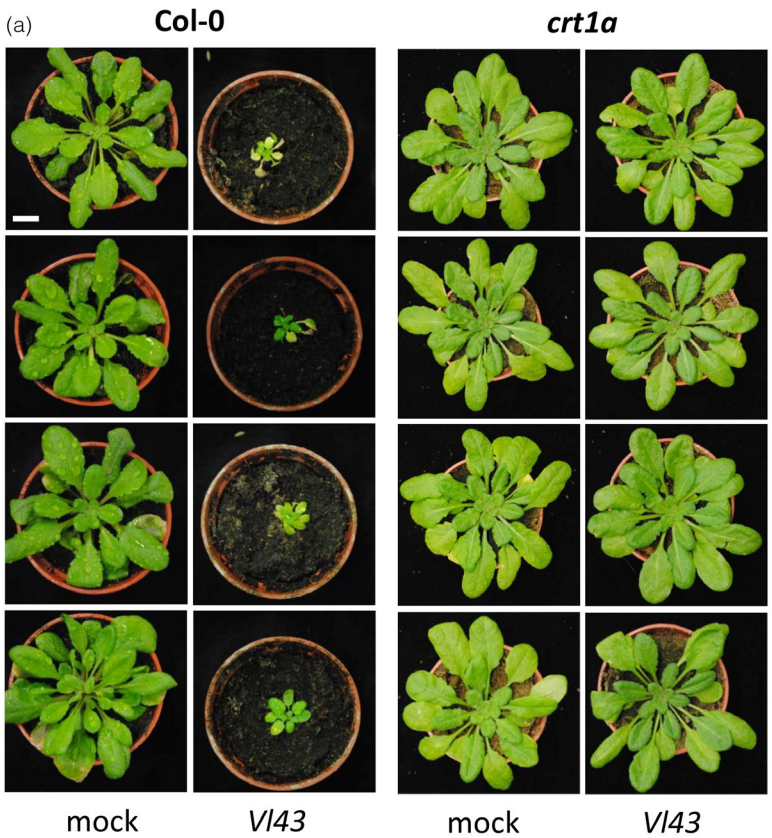


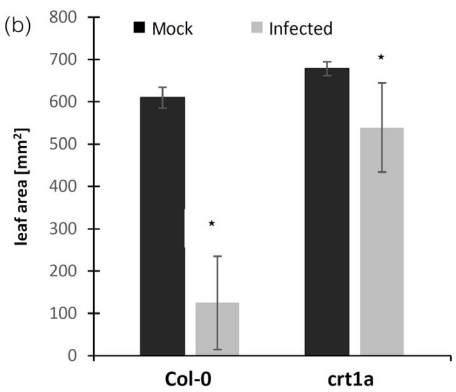


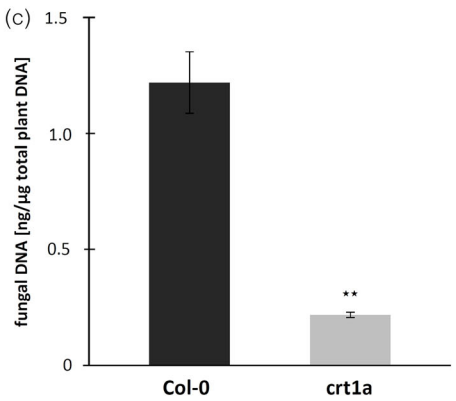


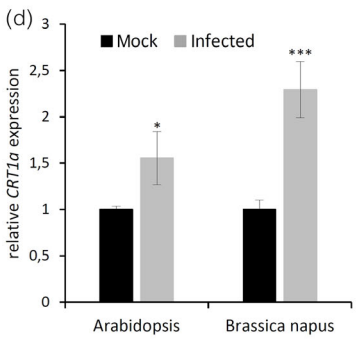


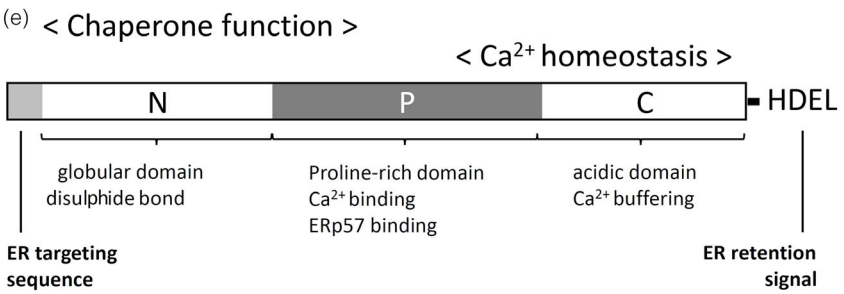


(f)

| CDS | amino acid | | | | |
|---|---|---|---|---|---|
| gene identifier | At1g56340 | BnaA09g15400 | BnaC09g16150 | BnaA09g15970 | BnaC01g43040 |
| At1g56340 | | 91.06 % | 91.29 % | 90.59 % | 90.65 % |
| BnaA09g15400 | 89.56 % | | 98.11 % | 94.58 % | 91.12 % |
| BnaC09g16150 | 89.67 % | 98.11 % | | 94.34 % | 92.06 % |
| BnaA09g15970 | 88.18 % | 93.02 % | 92.86 % | | 95.56 % |
| BnaC01g43040 | 87.49 % | 91.61 % | 91.53 % | 97.75 % | |

**Figure 1** The Arabidopsis CRT1a mutant displays reduced susceptibility to *VL43* infection. (a) Disease symptom development of crt1a as compared to Col-0 wild-type plants infected with $1 \times 10^6$ conidia/mL. Photographs were taken at 28 dpi. The scale bar equals 1 cm. (b) Leaf area analysis as measured at 35 dpi. (c) Fungal proliferation within infected Arabidopsis roots as measured by quantification of fungal DNA via qPCR at 28 dpi. (d) CRT1a is up-regulated in response to *Vl43* infection at 6 dpi in both in *Arabidopsis thaliana* (left) seedlings and *Brassica napus* (right) roots. (e) Typical calreticulin structure, according to Christensen *et al.*, 2008. (f) Comparison of Arabidopsis and *Brassica napus* CRT1a sequence homology on CDS and amino acid level. Numbers indicate the % identity. Statistical significance was determined on the basis of three independent biological replicates by Student's *t*-test and was evident for differences between wild-type and the respective mutants (*$P \leq 0.05$; **$P \leq 0.01$).

 

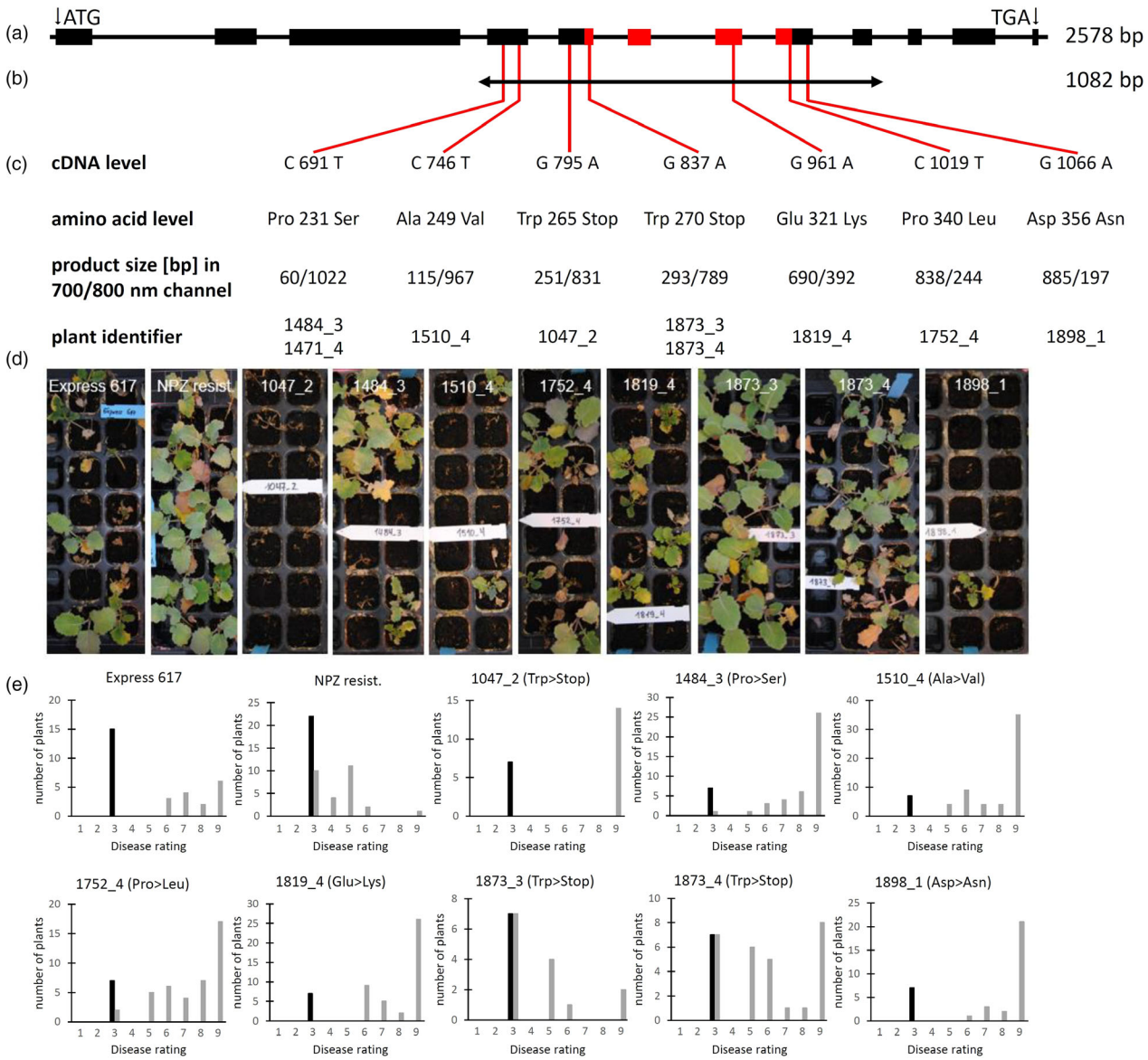


**Figure 2** TILLING analysis of the CRT1a locus BnaA09g15400D. (a) Genomic structure consisting of 12 exons (boxes) with the EST region identified in the SSH library indicated in red (see also Figure S4A). (b) Region selected for TILLING containing exons 4–9. (c) Location of mutations identified by TILLING according to the cDNA and amino acid level. (d) CRT1a oilseed rape TILLING mutants were infected with *Verticillium longisporum* in comparison with the susceptible line Express 617 and a less susceptible NPZ-resistant reference. Photographs were taken at 35 dpi. Squares are 4 × 4 cm. (e) Rating of disease symptoms. The disease rating was conducted according to Zeise and von Tiedemann (2002) and used to monitor disease severity in infected and non-infected oilseed rape plants. The rating is distributed from 1 (no symptoms) to 9 (dead plant).

survive the infection. This might be attributed to background mutations caused by EMS mutagenesis in the plant genome. To address the impact of background mutations on the decreased susceptibility observed in mutants 1873_3 and 1873_4, a successive backcross is in progress and genome editing using CRISPR/Cas was applied for a targeted CRT1a KO.

## Allele-specific mutations of *BnCRT1* by CRISPR/Cas

To exclude potential side effects from unwanted off-target background mutations frequently occurring by the EMS treatment, we employed the CRISPR/Cas technology for a target-specific mutation of the *BnCRT1a* loci. Thus, we constructed a vector, referred to as MP_23, by utilizing gene synthesis to obtain a codon-optimized Cas9 for *Brassica napus* (Figure S5). We designed a single sgRNA allowing to discriminate between 'on-target' (BnaA09g15400D and BnaC09g16150D) and 'off-target' (BnaA09g15970D and BnaC01g43040D, as well as all CRT1b copies) alleles. The BnaA09g15400D locus is the same as in the TILLING approach corresponding to the SSH library EST (6F11-F8). This is visualized in Figure 4A by a phylogenetic analysis in combination with the aligned target region (Figure 4B). In total, 20 independent transgenic oilseed rape plants were obtained, from which four T0 transformation events (C1 to C4) were identified as mutants carrying expected mutations in the target region as revealed by locus-specific sequencing (Figure 4C).

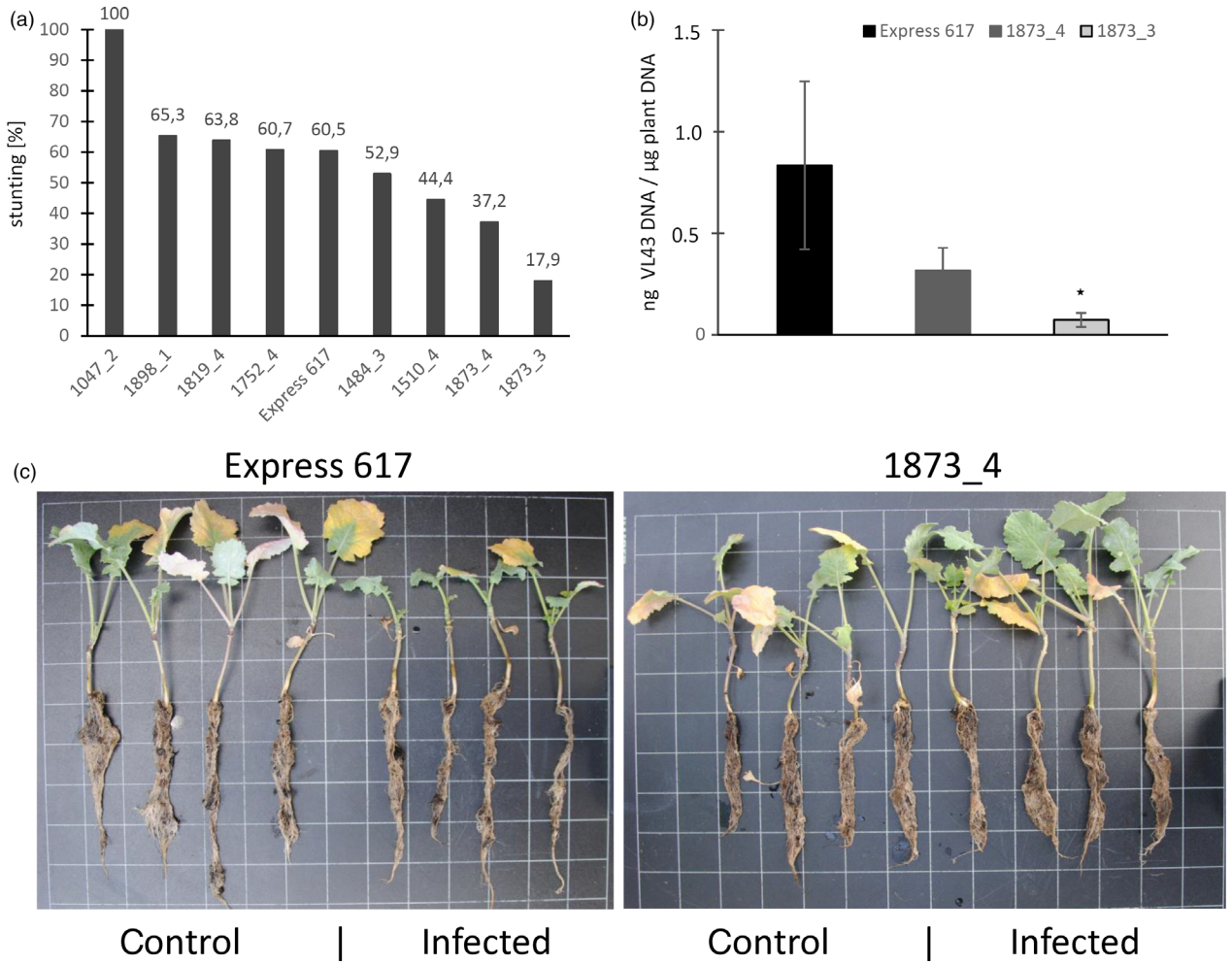


**Figure 3** Resistance phenotype of TILLING mutants. (a) Plant size reduction for infected oilseed rape candidates compared to the susceptible cultivar Express 617 at 35 dpi. With a 60.5% stunting degree, Express 617 is in the middle field among the investigated plants. 1484_3 and 1510_4, and above all 1873_4 and 1873_3 show clear reduction in stunting, demonstrating an enhanced resistance against *Vl43*. (b) Results of qPCR to quantify *Verticillium longisporum* DNA in roots of selected resistant oilseed rape mutants 1873_3 and 1873_4 at 42 dpi in comparison with the susceptible Express 617 cultivar. Significances were calculated using Student's *t*-test (*$P \leq 0.05$). (c) Disease phenotype of infected wild-type (Express 617) and mutant (1873_4) plants at 42 dpi. Squares are 3 × 3 cm.

For confirmation, genomic DNA of the four T0 plants was subsequently subjected to a 'derived cleaved amplified polymorphic sequence' (dCAPS) assay (Figure S6A/D). As expected, PCR fragments from wild-type plants were almost completely digested by *Pdm*I, while the T0 plants all showed partial digestions with varying intensities (Figure S6A), indicating varied mutation rates in the *BnCRT1a* alleles. Thus, this screening with the dCAPS assay is an efficient and a reliable tool to quickly identify CRISPR/Cas-derived mutations, especially for crops with complex genomes also proving that our CRISPR/Cas system is functional.

Next, the T1 and T2 generations for all four independent mutant events were analysed. To simplify the screening procedure, three T1 and T2 plants descending from each event were propagated and characterized at first by dCAPS to identify progenies with complete mutation of all BnCRT1a alleles. Figure S6B,C show examples of the progenies selected by dCAPS assay of the T1 and T2 individuals, demonstrating that mutations were stably transmitted to the T2 generation. The large insertion of 117 bp detected in the T0 event C4 was successfully deselected from progenies for further analysis since this mutation was in frame causing no potential KO. A complete mutation of the *BnCRT1a* locus was indicated only in the C1- and C4-derived T2 plants, while the C2 and C3 individuals showed still varied intensities of digestion patterns in the dCAPS assay (Figure S6C).

First, we challenged T2 plants with *Vl43* ($1 \times 10^6$ conidia) under greenhouse conditions and compared them with wild-type plants as control. Without fungal infection, most mutant plants showed no obvious difference in plant growth and development as compared to the control (Figure 5A). While at 28 dpi typical disease symptoms such as yellowing of leaves and stunting of plant growth appeared in the wild type, the mutant plants with the exception of plants derived from event C2 showed overall decreased disease symptoms as calculated by the area under the disease progress curve (AUDPC; Figure 5B), less stunting as measured by plant height (Figure 5C) when compared to the control. In particular, the T2 progenies derived from the T1 parents C3E3 and C4E23 showed a significantly reduced

 

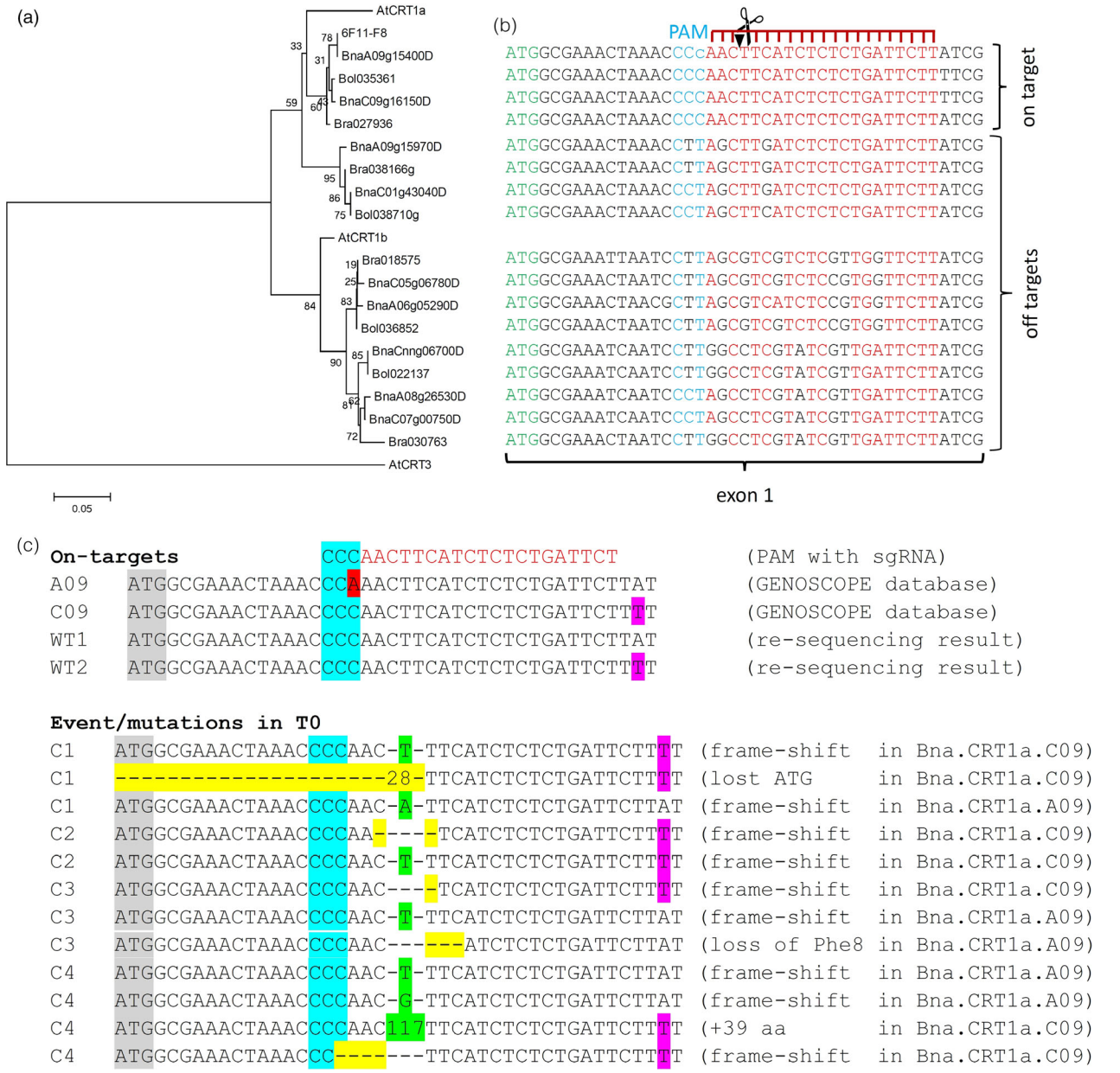


**Figure 4** Identification of CRISPR/Cas-induced mutations. (a) The neighbour-joining tree was based on corrected cDNA sequences and calculated with MEGA6 applying 1000 bootstraps, maximum composite Likelihood, d; uniform rates, same (homogenous); and complete settings and AtCRT3 as an outlier to root the tree. (b) CRT1a target region analysis. Shown is the beginning of exon 1, starting with the ATG (green letters). Only the two closely related CRT1a copies BnaA09g15400D and BnaC09g16150D are expected to be cleaved by the sgRNA guided Cas9, since other copies contain SNPs either in the PAM (blue letters) or the seed region of the sgRNA (red letters). (c) Detection of CRISPR/Cas-induced mutations in four independent T0 events (C1 to C4). Grey marks the start codon of the CRT1a ORF. Blue marks the PAM sequence of the Cas9-sgRNA. Insertions are coloured green and deletions in yellow. Purple indicates SNPs distinguishing copies from the AA and CC genomes and the red SNP a difference between database and re-sequencing results, but this has no negative impact on CRISPR/Cas specificity or functionality of the PAM (NGG).

susceptibility as indicated by impaired development of disease symptoms and less stunting (Figure 5D), as well as reduced fungal growth (Figure 5E). Even under a higher infection pressure with $1x10^7$ conidia, the mutants of C3E3 and C4E23 survived the infection until 28 dpi, while the control plants were completely deceased (Figures 5F left and S8).

Furthermore, there was no statistically significant difference in the 1000 corn weight between the T2 progenies from all four independent T0 events (Figure S7), indicating that the *crt1a* mutation has no negative effect on this agronomic trait. Though we observe a slight growth suppression after infection (Figure 5F right), the mock-treated C3E3 mutant plants grew similar to wild-type plants. Additionally, randomly chosen five individual plants were checked from each tested T2 population for the transgene construct by PCR and three plants appeared to be transgene-free (Figure S9).

In a next step, we genotyped T2 individuals by *BnCRT1a* locus-specific Sanger sequencing, including the off-target CRT1a alleles. On average, 40 clones per individual were analysed. No mutations were found in the off-target alleles (data not shown), while the detected mutations in BnaA09g15400D were mostly corresponding to those observed in the T0 generation (Figure 4C) with exception for C2E9-3 (Table 1). This indicates a stable inheritance of several CRISPR/Cas-induced mutations and confirms our observations from the dCAPS analysis (Figure S6C). Interestingly, we observed that the C2E9 plant harbours an intact allele of the BnaA09g15400D copy displaying the weakest phenotype with respect to the reduced susceptibility, while the C3E3 plant has two intact alleles of the closely related BnaC09g16150D copy but being most resistant, which is in agreement with our TILLING results. This suggests BnaA09g15400D is the 'active' *CRT1a* copy in *Brassica napus* being involved in the plant–fungus interaction.

A bioinformatic analysis (Blom *et al.*, 2004) suggests that two potential phosphorylation sites might be responsible for this difference between BnaA09g15400D and BnaC09g16150D, being present in the former and missing in the latter copy (Figure S10A). It appears that the first site was lost in BnaC09g16150D, while the second was gained in BnaA09g15400D (Figure S10B). Furthermore, the complete KO by frame-shift mutations as observed in C1E22 and C4E23 affecting all four BnCRT1a on-target alleles results in a less strong

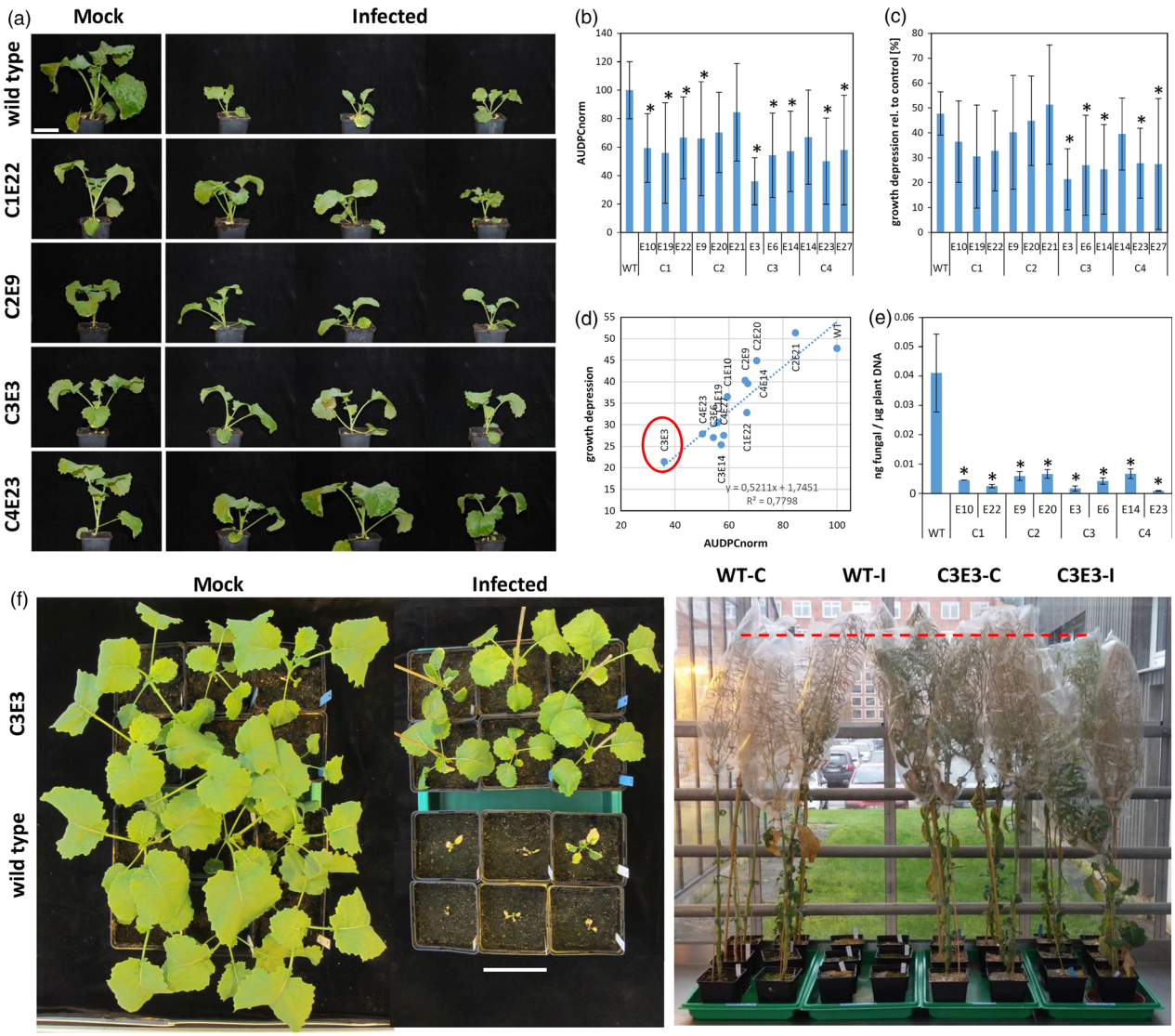


**Figure 5** CRT1a CRISPR mutants display reduced susceptibility. (a) T2 progenies of four independent events were photographed at 28 dpi with *Verticillium longisporum* (after infection with 1 × $10^6$ spores/mL). Some CRT1a mutants display better growth under infected conditions when compared to the wild type shown on top. The scale bar equals 9 cm. (b) Disease rating according to Eynck *et al.* (2007). The area under the disease progress curve (AUDPC) was determined starting at 7 dpi weekly until 28 dpi, and growth depression (c) was determined at 28 dpi and calculated from 10 individual plants. (d) Correlation analysis between (a) and (b) shows the best value for C3E3. (e) Fungal DNA was quantified via qPCR using the petioles of the first two true leaves harvested at 28 dpi. Statistical analysis was done by Dunnett's *t*-test, and significant changes are marked by asterisk (*$P \leq 0.05$). (f) The mutant C3E3 was infected a second time, now with 1 × $10^7$ spores/mL and photographed at 28 dpi (left) and after 21 weeks (right). The scale bar equals 13 cm.

phenotype, suggesting the type of mutation might also play a role. The 3-bp deletion observed in BnaA09g15400D of C3E3 causes loss of Phe8 within the N-terminal ER targeting sequence (Figure S10B) and might cause aberrant localization of CRT1a. Additionally, we still detected WT alleles in some T2 individuals (Table 1). Thus, it appears CRISPR/Cas becomes less active once plants were regenerated from callus culture, though we still observed Cas9 expression in T2 plants (data not shown).

### The ethylene pathway appears to be induced in the *crt1a* mutants

In order to get a first clue about the underlying molecular mechanism causing reduced susceptibility in the *crt1a* Arabidopsis and OSR mutant plants, we analysed the expression of several phytohormone marker genes involved in plant defence towards pathogens, such as PR1 (salicylic acid), PDF1.2 (jasmonic acid) and ETR2 (ethylene), as well as NCED3 for abscisic acid often involved in abiotic stress defence. Comparing wild-type and mutant backgrounds of Arabidopsis and OSR, we found no statistically significant differences for PR1, PDF1.2 and NCED3. However, for ETR2 we could observe an overall increase in OSR mutants, as well as in the Arabidopsis KO line when compared to the respective wild type (Figure 6A). Following this, we investigated several ET pathway-related genes in the highly resistant OSR mutant C3E3 and found that in addition to ETR2, also the expression of ACO1 and ERF73 was significantly elevated (Figure 6B/C).

## Discussion

In this study, we demonstrate a strategy and working routine allowing for an efficient generation of recessive resistance against pathogens in oilseed rape. By differential gene expression deploying a SSH library, we identified several putative candidates for susceptibility factors in the *Brassica napus–Verticillium longisporum* interaction. The related model plant *Arabidopsis thaliana* can be infected with *Vl43* as well. Thus, we obtained for 20 corresponding Arabidopsis orthologous gene loci T-DNA knockout lines and infected 15 homozygous mutants with *Vl43*. One loss-of-function mutant displaying increased resistance compared to the wild-type Col-0 was identified as *crt1a*. The T-DNA insertion into the Arabidopsis *CRT1a* gene resulted in decreased symptom development and fungal DNA accumulation, suggesting this might be a novel factor that plays an important role in the establishment of compatibility/successful host colonization by *V. longisporum*. For Col-0 wild-type plants, we observed a reduction in plant height of 41.9%, which was only 31.4% in *crt1a*, while the decrease in silique numbers reached 87.8% in wild-type plants compared to only 65.9% in *crt1a*. Also, the leaf area reduction was significantly less pronounced in *crt1a* when compared to infected Col-0 plants, and in consistence with these observations, we measured significantly less *Vl43* DNA in *crt1a* roots as compared to WT plants, suggesting that altered responses are mainly attributed to lower susceptibility towards *V. longisporum*.

**Table 1** Summary of detected mutations in on-target loci of T2 individuals

| Plant | *BnCTR1a* | Allele a | Allele b | Resistance level |
|---|---|---|---|---|
| C1E22 | BnaA09g15400D | +1 bp (A) | +1 bp (A) | ++ |
| | BnaC09g16150D | −28 bp | −4 bp | |
| C2E9 | BnaA09g15400D | WT | +1 bp (T) | + |
| | BnaC09g16150D | −4 bp | +1 bp (T) | |
| C3E3 | BnaA09g15400D | −3 bp (Phe8) | +1 bp (T) | +++ |
| | BnaC09g16150D | WT | WT | |
| C4E23 | BnaA09g15400D | +1 bp (T) | +1 bp (T) | ++ |
| | BnaC09g16150D | −4 bp | −4 bp | |

The characterization of Arabidopsis knockout mutants was followed by the identification of corresponding OSR mutants in an EMS-mutagenized population by TILLING. A database search at GENOSCOPE revealed four distinct CRT1a copies in the *Brassica napus* genome, all being expressed in cDNA preparations from infected and mock-treated roots (Figure S4B). We identified BnaA09g15400D as the *BnCRT1a* copy matching 100% to the EST identified from the SSH library. Thus, we focused on this CRT1a copy when designing specific TILLING primer. Nine OSR mutant candidates with single nucleotide mutations in the target locus (BnaA09g15400D) were identified. These mutations mostly led to amino acid changes in the protein (mis-sense mutation). Three lines with stop codons in the *CRT1a* ORF (potential knockouts) displayed converse phenotypes: the line 1047_2 was hyper-sensitive to *Vl43* infection, while the lines 1873_3 and 1873_4 appeared more resistant, suggesting strong side effects from the EMS mutational background. To clarify whether mutation of *BnCRT1a* really results in a decreased susceptibility to *Vl43* infection, a successive, time-consuming backcross is required. But in the light of legal issues concerning GMO regulations, the TILLING approach is still attractive since EMS-mutated plants are not regulated as transgenic GMOs (Henikoff *et al.*, 2004), while in Europe, SSN-mutated plants currently fall under GMO regulations (Urnov *et al.*, 2018).

Nevertheless, to verify the observed reduced susceptibility to *Vl43* in OSR, we applied CRISPR/Cas to specifically target the 'active' *CRT1a* locus BnaA09g15400D. We developed a CRISPR/Cas system optimized for *Brassica napus* and designed a sgRNA targeting BnaA09g15400D and also BnaC09g16150D, but not in the off-target CRT1a copies BnaA09g15970D and BnaC01g43040D. It is interesting to note that several of the identified mutations were identical between the T0 and T2 plants (Figure 4C and Table 1) and that even though CRISPR/Cas is assumed not to rest unless all target loci are mutated, still some wild-type alleles could be found in two sequenced individuals. This indicates that CRISPR/Cas-induced mutations did not generally increase over two generations, albeit Cas9 was still expressed in T2 plants (data not shown). One explanation might be that the construct is mainly active during tissue culturing, an observation also made by others (Mikami *et al.*, 2015). Alternatively, such incomplete mutation might be due to certain epigenetic modification at the target loci (Kallimasioti-Paz et al., 2018; Verkuijl and Rots, 2019).

It is to note that plants of C3E3 and C4E23 displayed a stronger mutation effect, even under a higher infection pressure with $10^{-7}$ spores/mL as *Vl43* inoculum (Figures 5F and S9). The mutations in the C3E3 plants affected only the 'active' TILLING copy BnaA09g15400D, while in C4E23 plants, both on-target copies were mutated. Though C2E9 plants are completely mutated in the BnaC09g16150D copy, they showed the weakest resistance phenotype, suggesting this copy is less important

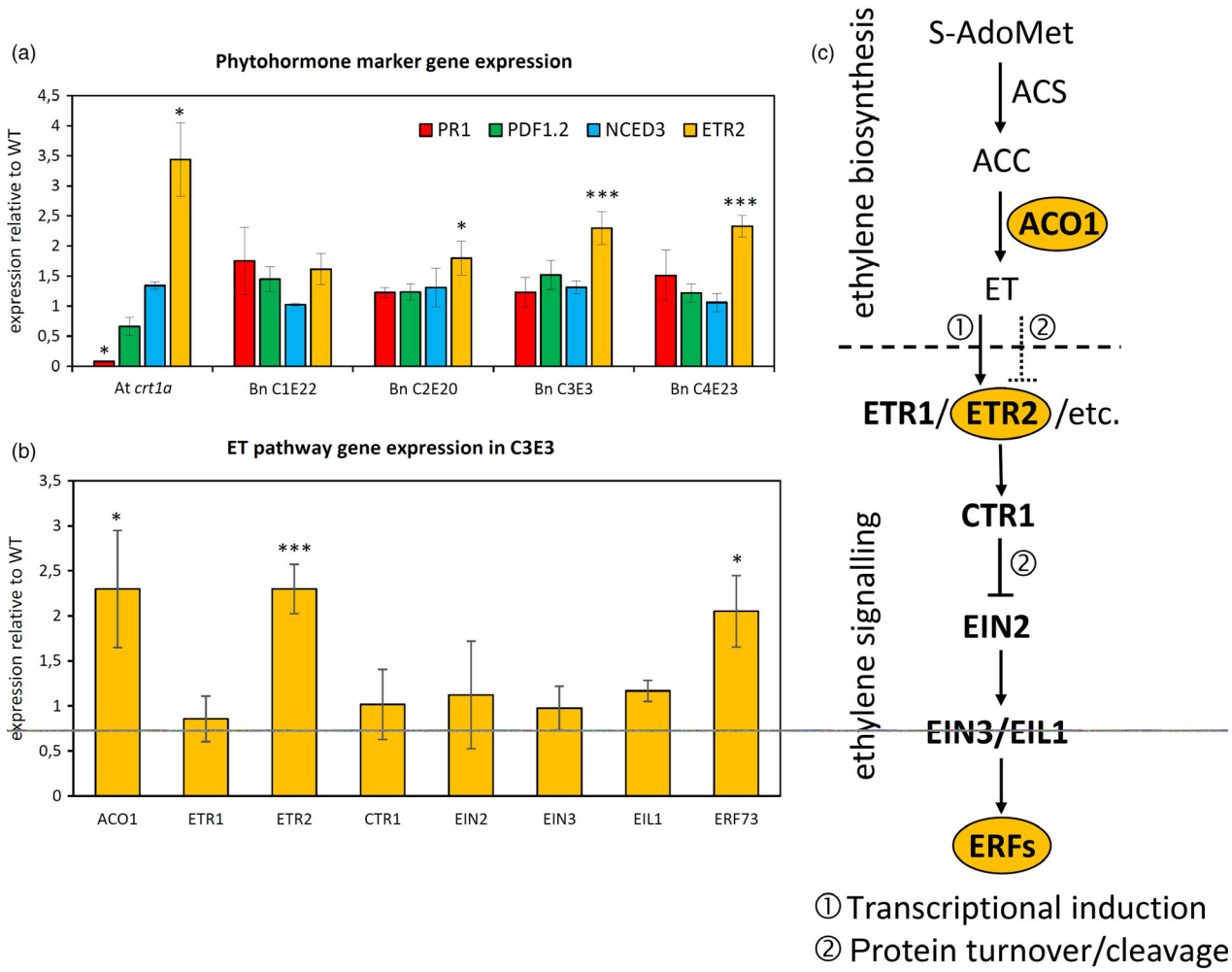


**Figure 6** Up-regulation of the ethylene pathway in *crt1a* mutants. (a) Marker gene expression analysis by qPCR relative to wild type. Expression of PR1 for the salicylic acid pathway, PDF1.2 for the jasmonic acid pathway, NCED3 for abscisic acid and ETR2 for the ethylene pathway was investigated in both Arabidopsis *crt1a* (SALK_055452) and several OSR *crt1a* mutant backgrounds. (b) ET gene expression analysis in C3E3 plants by qPCR relative to wild type. Root material was harvested from 4-week-old Arabidopsis plants and 2-week-old *Brassica napus* plants. Statistical significance was checked on the basis of three independent biological replicates by Student's *t*-test (*$P \leq 0.05$; **$P \leq 0.01$). (c) Simplified overview of the ET signalling pathway in plants (modified from Ju and Chang, 2015).

(Table 1). This might be explained by differences at the amino acid level between both on-target copies. An *in silico* analysis reveals that BnaA09g15400D contains two potential phosphorylation sites, which are missing in BnaC09g16150D (Figure S10A). Furthermore, it appears that the first site was lost in BnaC09g16150D, while the second was gained in BnaA09g15400D (Figure S10B). But in how far this affects CRT1a function still remains to be elucidated. Thus, we conclude that the BnaA09g15400D copy is a dominant functional homeolog being important for the plant–fungus interaction and that its loss of function impedes the compatible interaction and reduces plant susceptibility to *Vl43*. In addition, five T2 progenies for each selected T1 plant (Figure S9A) were tested by PCR for the presence of the CRISPR/Cas construct. From them, three plants appeared to be transgene-free (Figure S9B). Thus, we believe that it is possible to generate transgene-free plants carrying only the mutation in the target locus already in T2 generation. Analysis of the 1000 seed weight showed additionally that the CRISPR/Cas-mutated *crt1a* lines were not negatively affected in comparison with the wild-type Mozart (Figure S7).

The finding that CRT1a knockout results in decreased susceptibility to *Vl43* in two *Brassicaceae* species, *Arabidopsis thaliana* and OSR, strongly supports the importance of CRT1a in a compatible plant–fungus interaction. It is to note that the C3E3 mutant lacks only Phe8 in one BnaA09g15400D allele but confers higher resistance than the other mutants (Figure 5F). We speculate that this mutation might impair the ER targeting of CRT1a, resulting in an atypical allocation of the protein in plant cells, and that the still-intact BnaC09g16150D alleles compensate for some other CRT1a function in plant resistance. Calreticulin (CRT) was initially described from rabbit skeletal muscle sarcoplasmic reticulum serving as a $Ca^{2+}$ binding protein (Ostwald and MacLennan, 1974). This highly conserved protein is found in higher eukaryotes and locates to the endoplasmic reticulum (ER), where it is involved in the regulation of many cellular processes (Krause and Michalak, 1997). Plant CRTs were first isolated from spinach and tobacco (Denecke *et al.*, 1995; Menegazzi *et al.*, 1993) and in *Arabidopsis*

*thaliana* exist three CRT family members (CRT1a, 1b and CRT3), which share protein sequence similarities from of 57%–86%. The predicted amino acid sequences of plant calreticulins have structural similarities to those found in animals (Coppolino and Dedhar, 1998), and it was shown that AtCRT1a could substitute the chaperone and $Ca^{2+}$- homeostasis function of animal CRTs, indicating that basic functions are conserved between the two kingdoms (Christensen *et al.*, 2008). Since CRTs are ubiquitously expressed, it is supposed that they play a general role in plant growth and developmental processes (Jia *et al.*, 2009). Structurally, calreticulins contain three different domains, which are the N-terminal globular domain with chaperone function, a central proline-rich domain for high-affinity $Ca^{2+}$ binding adding to the chaperone function and a C-terminal acidic domain responsible for $Ca^{2+}$ buffering with a C-terminal ER retention signal (Sarwat and Tuteja, 2017). It appears that isoform CRTs have different functions, for example CRT3 being distinct from CRT1a and 1b, which are in contrast co-expressed with a multitude of ER genes (Christensen *et al.*, 2010; Jia *et al.*, 2009).

Besides their role in calcium regulation, CRTs are involved in the ER quality control, functioning as chaperones to ensure proper protein folding (Danilczyk *et al.*, 2000) and this has also an impact on abiotic and biotic stress responses (Garg *et al.*, 2015, Kang *et al.*, 2010). For example, the Arabidopsis triple mutant of CRT1a, CRT1b and CRT3 showed growth defects in response to water stress, suggesting that CRTs are involved in drought stress responses. The absence of defects in single isoform mutants could be explained by compensation of certain functions because of functional redundancy (Kim *et al.*, 2013). Other potential roles of plant CRTs in abiotic and biotic stress responses have been recently reviewed (Joshi *et al.*, 2019). For biotic stress, tobacco calreticulin was shown to be involved in cell-to-cell movement of TMV (Chen *et al.*, 2005) and it has been shown that CRT3 plays a role in folding of EFR (but not FLS2), establishing also a link to induction of PAMP-triggered immunity (Christensen *et al.*, 2010; Li *et al.*, 2009). A knockdown of CRTs led to a disturbance of the Ve1-mediated resistance against *Verticillium dahliae* in tomato, indicating a function in proper folding of Ve1 receptor-like protein (Liebrand *et al*., 2014). Thus, it is reasonable to speculate that the loss of CRT1a function could also result in an indirect effect leading to misfolding and degradation of other susceptibility factors, which are then absent and therefore impede pathogen development.

Such impaired ER quality control by CRT1a loss of function could furthermore prevent correct folding of negative regulators in ethylene (ET) signalling, since we observed up-regulation of the ET-responsive gene *ETR2* in *crt1a* roots (Figure 6A) and a constitutively activated ET signalling pathway might contribute to *VL43* resistance, as has been shown also for other pathogenic fungi infecting roots (Okubara and Paulitz, 2005). Interestingly, ETR2 is one of five ET receptors located in the ER and regulated by MAPK (mitogen-activated protein kinase) cascades (Das *et al.*, 2015; Shakeel *et al.*, 2015) and itself involved in negative regulation of the ET-activated signalling pathway *via* ET perception (Ju and Chang, 2015). *ETR2* is transcriptionally activated in response to ET, but the protein is also degraded after ET perception (Chen *et al.*, 2007; Shakeel *et al.*, 2015). Concerning ETR2 expression, we could observe a dose effect in OSR roots, being highest in the more resistant lines C3E3 and C4E23 (Figure 6A). We investigated transcriptional activation of several ET pathway genes in the C3E3 mutant, and besides, *ETR2* only ACO1 and ERF73 were significantly up-regulated (Figure 6B). This is not surprising since ET signalling is largely regulated post-transcriptionally by protein modification and degradation (Gallie, 2015; Merchante *et al.*, 2013). An at least partially induced ET pathway would imply a fundamental change in the plants alert status, which might also explain to some extend why *crt1a* mutants become less susceptible. That ET can contribute to the plant defence towards *Verticillium* ssp. is further corroborated by observations that *V. dahliae* degrades the ET precursor 1-aminocyclopropane-1-carboxylic (ACC) to increase its virulence, while ACC pretreatment reduced symptoms in tomato (Tsolakidou *et al.*, 2019). Very recently, Xiong *et al.* (2020) reported that a knockdown of GhWRKY70D13 improved cotton resistance to *V. dahliae* going along with up-regulation of genes involved in ET and jasmonic acid (JA) biosynthesis as well as increased ACC, JA and JA-isoleucine levels. Also, Arabidopsis ERF TFs are induced in response to *V. longisporum* and their over-expression caused a reduction of fungal DNA within the mutants, while RNAi against ERFs had the opposite effect (Fröschel *et al.*, 2019). But also the opposite effect has been observed with Arabidopsis *etr1* mutants being more resistant to *V. dahliae* (Pantelides *et al.*, 2010). However, the constitutively expressed ETR1 is not responsive to ET and has a higher affinity for CTR1 as compared to ETR2, pointing to different functional roles (Chen *et al.*, 2007; Shakeel *et al.*, 2015). For example, ETR1 and ETR2 act reversely in abscisic acid-mediated seed germination under salt stress (Wilson *et al.*, 2014). In summary, we demonstrate a strategy and working routine to increase natural variation for improving plant disease resistance in OSR. Following this, we identified CRT1a as a novel susceptibility factor, which loss of function reduces OSR and also Arabidopsis susceptibility to *V. longisporum* without negatively affecting overall plant performance under greenhouse conditions, being therefore a potentially interesting target for breeding programmes.

## Material and Methods

### Fungal cultivation

*Verticillium longisporum* isolate *Vl43* provided by Dr. Elke Diederichsen (FU Berlin, Germany) was stored as 22% glycerol stock culture and conidia were produced by transferring mycelium plugs from one-week-old PDA (Duchefa, the Netherlands) plates into liquid Czapek-Dox (Duchefa, the Netherlands) medium for subculturing in the dark at 25 °C on a rotating shaker. After 1 week, conidia were harvested with the help of gaze filter (mesh 200 μm; Hydro-Bios Kiel, Germany), centrifuged for 8 min at 8000 rpm and resuspended in sterile Czapek-Dox medium to increase the concentration. Stocks for infection were supplemented with 86% glycerol to a final concentration of 22% and kept at −80°C till the day of inoculation. At the day of inoculation, stocks were thawed, centrifuged for 8 min at 8000 rpm and resuspended in tap water (for '*in vivo*' infection on soil) or sterile Czapek-Dox medium (for '*in vitro*' infection) to a final concentration of $1 \times 10^6$ conidia/mL if not otherwise indicated. Tap water and Czapek-Dox medium were used as mock treatments, respectively.

### Plant material and growth

Arabidopsis and *B. napus* seeds were surface-sterilized with a 6% sodium hypochlorite/Tween-20 solution and 70% ethanol followed by three times washing with sterile dist. water. The Arabidopsis ecotype Col-0 (wild type) was purchased from Lehle Seeds, Round Rock, TX, USA, while T-DNA insertion mutants

were obtained from NASC, Nottingham, UK. Homozygous plants were selected using the T-DNA-specific primer LBb1.3 (http://signal.salk.edu/tdnaprimers.2.html) in combination with locus-specific primers (Table S6). Surface-sterilized seeds were placed in B5 agar medium and grown under short-day conditions (8-h light/16-h dark) at 22 °C in a growth chamber for four weeks. Seeds of the susceptible OSR cultivar 'Express 617', a NPZ-resistant reference line and the TILLING mutants were provided by the Norddeutsche Pflanzenzucht Hans-Georg Lembke KG (NPZ). Surface-sterilized seeds were placed on B5 agar medium and grown under sterile long-day conditions (16-h light/ 8-h dark) at 22 °C in a growth chamber for 10 days.

### *In vivo* infection of *Brassica napus*

Seeds of *Brassica napus* were surface-sterilized with 70% ethanol and a 5% sodium hypochlorite solution with a drop Tween-20 followed by three times washing with sterile dist. water. They were sown out on sterile 1-mm-thick filter paper saturated with MS media without sucrose and placed into a climate cabinet (Vötsch VB 0714-A, Reiskirchen, Germany) with short-day conditions at room temperature. When the cotyledons were fully expanded after 7 days' incubation, *V. longisporum* stock culture was thawed on ice and then centrifuged at 6000 ***g*** for 10 min. The supernatant was discarded, and the pellet was dissolved in with the same amount of tap water. Roots of the *Brassica napus* seedling were cut with a razor blade to a length of 2 cm, and inoculation was performed according to Eynck *et al.* (2007) by the root-dip method using $1 \times 10^6$ conidia for mild infection or $1 \times 10^7$ conidia for strong infection. After inoculation for 5 min, plants were transferred to soil with an initial application of WUXAL® universal fertilizer (Bayer CropScience, Leverkusen, Germany) and grown under long-day conditions in the greenhouse until the day of harvest.

### *In vitro* Infection assay of *Brassica napus*

Seeds of *Brassica napus* were surface-sterilized with 70% ethanol and a 5% sodium hypochlorite solution with a drop Tween-20 followed by three times washing with sterile dist. water. The seeds were placed in plastic salad boxes with solid MS media and grown under short-day conditions until the cotyledons were fully expanded. Seedlings were transferred to 120 mm square Petri dishes containing ½ MS (0.5% sucrose) as described by Behrens *et al.* (2019). Roots were inoculated by brushing them with *V. longisporum* conidia suspension, and plants were grown under short-day conditions for six days in a climate cabinet (Vötsch VB 0714-A) with short-day conditions at room temperature. The root material was harvested, frozen in liquid nitrogen and stored at −80 °C until used for RNA isolation for gene expression studies.

### *In vivo* infection of *Arabidopsis thaliana*

Inoculation was performed according to Eynck *et al.* (2007) by the root-dip method for plants grown on soil. Arabidopsis plants grown under short-day conditions for 3 weeks in a climate cabinet (Vötsch VB 0714-A) were dipped for 5 min into a conidia suspension with different concentrations ($1 \times 10^3$ to $1 \times 10^7$ conidia/mL). Control plants were dipped for the same time into filtrated and autoclaved tap water. Immediately after the inoculation, plants were transferred into pots filled with a sand:vermiculite:soil mixture in a ratio 3:1:1, and additionally, 5 mL from the conidia suspension was given directly to each plant. The plants were photographed at the indicated time points, and roots were harvested at 28 dpi, flash-frozen in liquid nitrogen and stored at −80 °C.

### DNA and RNA isolation

Leaf and root tissue of at least three independent biological replicates from each infected and mock-treated plants was flash-frozen in liquid nitrogen and stored at −80 °C. DNA was isolated using the cetyltrimethylammonium bromide (CTAB) method (Rogers and Bendich, 1985), and the resulting DNA pellet was resolved in 50 μg $ddH_2O$, treated with RNaseI (Fermentas) for 1 h by 37 °C and stored at −20 °C until further use.

Total RNA was isolated using the TRIzol® Reagent (Invitrogen, Karlsruhe, Germany) according to the manufacturer's recommendation including a DNaseI (Fermentas, Vilnius, Lithuania) treatment. The resulting RNA pellet was resolved in 20–50 μL DEPC-treated $ddH_2O$ and stored at −20 °C until further use.

### Suppression subtractive hybridization (SSH library)

For the construction of the SSH libraries, mRNA was isolated with the 'PolyATract® mRNA Isolation System III' (Promega, Madison, Wisconsin) according to the manufacturer's instructions. After *Vl43* infection *B. napus* root material was collected at 5 dpi, 10 dpi and 15 dpi. Total RNA from the three harvesting time points was pooled into infected and mock-treated samples. The RNA quality and quantity was measured with the NanoVue Spectrophotometer (GE Healthcare, Chicago, Illinois) and by electrophoresis on agarose denaturing gel.

A forward (up-regulated genes after infection) and reverse (down-regulated genes after infection) SSH library was constructed using the PCR-select cDNA subtractive kit (ClonTech, TaKaRa Biotech, Saint-Germain-en-Laye, France) according to the manufacturer's manual from infected and non-infected *B. napus* root mRNA at the three harvesting time points 5 dpi, 10 dpi and 15 dpi. The pooled mRNA of infected and non-infected *B. napus* root was used. For the forward library, mRNA of non-infected roots was used as the driver, and the mRNA of infected roots was used as the tester. For the reverse library, tester and driver were changed. Double-stranded cDNAs were obtained according to the manufacturer's instructions and then used to initiate SSH procedure. Both, tester and driver were incubated for 1 h at 37 °C with *Rsa*I. Adapter 1 was ligated with half of the digested tester cDNA, and adapter 2R was ligated with the other half. Adequate driver cDNA was mixed with both of them in separate tubes for the first subtractive hybridization. The resulted products were mixed together, freshly denaturated driver cDNA was added, and the second subtractive hybridization took place. To enrich the differential expression fragment, PCR amplification was conducted.

To construct the SSH-cDNA library, the purified differentially expressed fragments were cloned into pGEM®-T Easy Vector (Promega) and transformed into electrocompetent *Escherichia coli* strain DH5α (Invitrogen), cultured on LB medium containing Amp/IPTG/X-Gal for blue-white screening at 37 °C. Positive clones were selected on new LB medium, grown overnight at 37 °C and analysed by PCR with vector-specific standard primer pairs SP6/T7 or M13F/M13R (both Invitrogen). Positive clones were sent for sequencing. PCRs were carried out in a total volume of 20 μL with 10 pmol for each primer, 10 mM PCR buffer (pH 8.3), 1 U of Taq DNA polymerase (Invitrogen), 2 mM $MgCl_2$ and each dNTP at 5 mM in a standard thermocycler (Biometra, Göttingen, Germany). PCR was performed using a PCR

 

programme of 94 °C for 1 min, 56 °C for 30 s and 72 °C for 30 s for 35 cycles, followed by 5 min at 72 °C.

Sequences from the SSH clones were determined by the Department for Clinical Molecular biology at the University of Kiel, and sequence analysis was carried out using the software CHROMAS Lite (Technelysium Pty Ltd, South Brisbane, Australia). The obtained EST sequences from the suppressive subtractive hybridization were blasted at the NCBI database (http://blast.ncbi.nlm.nih.gov/Blast.cgi) using the BLASTX algorithm (Altschul *et al.*, 1990) and TAIR10 database for Arabidopsis (Berardini *et al.*, 2015).

### Phylogenetic analysis

A neighbour-joining phylogenetic tree based on corrected cDNA sequences of *CRT1a* and *CRT1b* was created using MEGA6 software (Tamura *et al.*, 2013). The tree was calculated by applying 1000 bootstraps with the following settings: maximum composite likelihood, d; uniform rates, same (homogenous). *AtCRT3* was included as an outlier to root the tree.

### TILLING

The sequence of *CRT1a* (AT1G56340) was retrieved from the Arabidopsis database TAIR (The Arabidopsis Information Resource) and submitted to BLAST analysis at the GENOSCOPE *B. napus* database (http://www.genoscope.cns.fr/brassicanapus). Additionally, homologous genomic sequences from the Brassica database (BRAD) for *B. rapa* and *B. oleracea* were retrieved as well. A sequence alignment was performed comparing all sequences with the *CRT1a* EST, which was found in our comparative transcriptome analysis, matching 100% to the 'active copy' (BnaA09g15400D). Gene copy-specific primers were designed to amplify 1082 bp, covering 41.7% of the *CRT1a* ORF (Table S5). Gene-specific primers, as well as fluorescence-labelled primers, were tested according to the protocol of Till *et al.* (2006), before the actual TILLING procedure started.

DNA samples from an EMS treated OSR $M_2$ population were provided by AG Prof. Dr. Jung, Institute of Plant Breeding, Christian-Albrechts-University of Kiel. In total, 3840 $M_2$ individual plant DNAs, pooled in ten microtitre plates, were employed in the TILLING screening as described in Harloff *et al.* (2012). Obtained DNA bands were extracted from the gel after electrophoresis and purified with the NucleoSpin® Gel and PCR Clean-up Kit (Macherey-Nagel, Düren, Germany). The locus specificity was confirmed by Sanger sequencing. The TILLING PCR of DNA pools was performed using 96-well plates (Bio-Rad) and CFX96 Touch™ Real-Time Detection System (Bio-Rad, Hercules, California). A mixture of unlabelled and 5′-end labelled (DY-681 and DY-781) forward and reverse primers was used for amplification, utilizing the proofreading Phusion High-Fidelity DNA Polymerase (Thermo Fisher Scientific, Waltham, MA, USA) and the following PCR programme: 95 °C 5 min, 40 cycles of 95 °C 30 s, 62 °C 30 s, 72 °C 90 s, 72 °C 10 min. Portions of the amplicon were checked by gel electrophoresis to confirm product specificity.

According to Till *et al.* (2006), the PCR products of mutated (EMS) plants and non-mutated (WT) plants were hybridized to form heteroduplex structures and celery juice extract was prepared from commercial celery. This juice extract contains CEL1, a heteroduplex-specific restriction endonuclease, which cuts DNA exactly at base-pair mismatch sites. The digestion was stopped with 50 mM EDTA. Samples were cleaned from salts and buffer residues by Sephadex gel purification. The sample volume was reduced by evaporation on a heat block at 90 °C. The IRD fluorescence-labelled PCR products were separated on polyacrylamide gels by using a LI-COR 4300 DNA analyser (LI-COR Bioscience) tool (4 h at 1.500 V, 40 mA and 40 W). Gel images were studied by the freely available software GelBuddy. After the identification of positive mutation signals in a DNA pool, corresponding single plant DNAs were used to confirm the single nucleotide mutation by Sanger sequencing (IKMB, Kiel, Germany). For sequencing, two independent PCRs were performed. The products were gel-purified with the NucleoSpin® Gel and PCR Clean-up Kit (Macherey-Nagel) and ligated into pGEM®-T Easy Vector System (Promega) according to the manufacturer's instructions. The T-Vector was transformed into heat shock-competent *E. coli* DH5α cells, and bacteria were selected on LB plates containing IPTG/X-gal and ampicillin. Positive clones were identified by blue-white screening. Plasmid DNA was isolated and sequenced using standard vector primers M13/T7. The obtained sequences were aligned with the specific *B. napus* gene copy by using CLUSTALW to identify nucleotide exchanges, allowing also the exact localization of the single nucleotide mutation in *CRT1a*. Visible double spikes in the electropherograms indicate that the plant is heterozygous for the corresponding point mutation. Unambiguous single peaks indicate homozygosity. Plants with homozygous genetic background were kept for seed production.

### dCAPS assay

Derived cleaved amplified polymorphic sequences (dCAPS) is a simple technique to genetically analyse nucleotide polymorphisms (Neff *et al.*, 1998). dCAPS is an alternative if the target region of sgRNA-directed CRISPR/Cas does not contain a natural restriction site to quickly screen for mutational events. In case of the CRT1a loci, primers have been designed (Table S6) to generate an artificial *Pdm*I restriction site, which would not be cleaved if the locus was successfully mutated, while wild-type sequences are cleaved into 29- and 63-bp fragments. The PCR products were digested with FastDigest *Pdm*I (Thermo Fisher Scientific) for 1 h before heat inactivation at 80 °C for 20 min and analysis by gel electrophoresis on a 2% agarose gel.

### *Vl43* gDNA detection in plant tissue

Arabidopsis roots and *B. napus* petioles from infected and mock-treated plants were sampled at the indicated time points and further processed as described in Behrens *et al.* (2019).

### Assessment of projected leaf area

The leaf area analysis was used to compare the leaf rosettes of control and *Vl43*-inoculated Arabidopsis mutant and wild-type plants. The plants were grown and infected in a 60-mm pot. After infection, the plants were photographed once a week in a precisely defined distance with a digital camera (Canon EOS 450D). The program WinCAM 2004a (Regent Instruments) was used to analyse the leaf area. A 1 cm × 1 cm white square served as scale to calculate the pixel area of the visible surface.

### Disease rating and AUDPC calculation

The scoring of disease symptoms was conducted according to Eynck *et al.* (2007) with a rating scale from 1 to 9 as shown in Table S7.

Symptoms of the *Vl43* infection of *Brassica napus* CRISPR/Cas mutants were assessed every 7 days until 28 dpi. From disease severity values, the area under the disease progress curve (AUDPC) values were calculated according to Campbell and Madden (1990):

$$\sum_{i=1}^{n} = \left(\frac{y_i + y_{i+1}}{2}\right) \times (t_{i+1} - t_i)$$

where $y_i$ = disease score for observation number $i$; $t_i$ = days postinoculation, $n$ = number of observations.

Adjusted AUDPC values were calculated to not overestimate the disease severity of each inoculated variant through natural occurring senescence. Therefore, AUDPC values from the mock control were subtracted from the AUDPC values from inoculated plants resulting in the $AUDPC_{net}$ values:

$$AUDPC_{net} = AUDPC\ (X_{inoc.}) - AUDPC\ (X_{contr.})$$

The $AUDPC_{net}$ values of each accession were further normalized against the WT resulting in $AUDPC_{norm}$ values. In addition to the AUDPC values, the plant height was measured at each scoring date as well. The growth depression (GD) compared to the mock control was calculated by dividing the plant height of the infected variant through the mock variant of each accession:

$$GD = \left(1 - \left(\frac{\text{Mean plant height}_{mock}}{\text{Mean plant height}_{infected}}\right)\right) \times 100$$

### cDNA synthesis and gene expression analysis by qRT-PCR

One μg of total RNA was deployed in first-strand cDNA synthesis, diluted in a ratio 1:10 and subjected to qPCR analysis as described in Behrens *et al.* (2019). For *Brassica napus*, the reference genes Bn-ß-tubulin 4 (224 bp) and BnActin 7 (216 bp) served as control, while in Arabidopsis, AtActin2 (298 bp) and AtPP2A (208 bp) were used as housekeeping genes. The primer sequences for all genes analysed can be found in Table S6.

### CRISPR/Cas

The *Brassica napus* reference genome used for all *in silico* analysis and sgRNA design was accessed *via* the GENOSCOPE Darmor-bzh v4.1 database (Chalhoub *et al.*, 2014). Annotated genes were obtained from the respective database, and the following genes served as template for sgRNA design conducted using the web tool Cas-Designer (Bae *et al.*, 2014; Park *et al.*, 2015). The PAM type was set to 5′-NGG-3′ (Cas9) and guide sequences with a hit in both *B. napus* target alleles, with localization at the beginning of the ORF within exons, were chosen as good candidates for sgRNA design. For *B. napus* a separate off-target analysis was conducted using the sgRNA target sequence and a second reference genome. Only hits present in both genomes were considered potential off-targets. The sgRNA was created according to Li *et al.* (2013) involving three rounds of PCR to replace the guide sequence within the sgRNA template (Figure S5) and expressed under the Arabidopsis U6-26 promoter described by Schiml *et al.* (2014).

To efficiently apply CRISPR/Cas to *Brassica napus* we established a vector system involving a codon-optimized Cas9 (http://www.kazusa.or.jp/codon/cgi-bin/showcodon.cgi?species=3708) with a C-terminal Mammalian Importin alpha type nucleus localization sequence (NLS). The entry vector for gateway cloning (BS_01) was synthesized based on a pUC57 backbone containing a sgRNA template driven by an AtU6 promoter within a multiple cloning site and the Cas9-NLS under the control of the CaMV 35S promoter. The recombination sites allow a gateway LR reaction to clone the CRISPR/Cas components into the binary vector pGWB401 (Nakagawa *et al.*, 2007), adding the NOS terminator to the Cas9-NLS and the nptII plant selection marker (kanamycin resistance). This resulted in the plant transformation vector MP_23, ready for *Agrobacterium tumefaciens*-mediated gene transfer (Figure S5). Stable transgenic lines were produced by the Saaten-Union Biotec GmbH (Leopoldshöhe, Germany).

### Statistical analyses

Graphs and plots were created with Microsoft® Office Excel® 2016 and statistical calculations were carried out in R. Simple comparisons of means for only two groups were done using the Student's or Dunnett *t*-test (*$P \leq 0.05$; **$P \leq 0.01$; ***$P \leq 0.001$).

## Acknowledgements

We thank Dr. Hans Harloff and Prof. Dr. Christian Jung from the Plant Breeding Institute at the Christian-Albrechts-University Kiel and our industry partner Norddeutsche Pflanzenzucht Hans-Georg Lembke KG and NPZ Innovation GmbH, Germany, for support with the TILLING material and equipment. For technical assistance in the greenhouse, we thank Christin Belz and Martina Wittke. Furthermore, we thank the Bundesministerium für Ernährung und Landwirtschaft (BMEL, Grant no. 22006516), the Bundesanstalt für Landwirtschaft und Ernährung (BLE, Grant No. 2814IP004), and the Bundesministerium für Bildung und Forschung (BMBF, Grant no. 031B0033C), Germany, for financial support.

## Conflicts of interest

There is no conflict of interest.

## Author contributions

Dirk Schenke: Bioinformatic analysis, gene expression analysis, design of CRISPR vector system, sequencing of target loci, data interpretation, arrangement of data, confirmation of CRISPR results, drafting and writing of manuscript. Michael Pröbsting: OSR CRISPR: sgRNA design to target BnCRT1a, cloning, transformation, dCAPS analysis, phenotyping of CRISPR mutants, sequencing of target loci, gene expression analysis. Roxana Hossain: Arabidopsis phenotype confirmation, gene expression analysis, OSR TILLING: Identification of mutations, sequencing of target loci. Claudia Häder: Establishment of pathosystem, SSH library analysis, selection of candidate genes, Arabidopsis mutant genotyping and pre-screening, gene expression analysis. Tim Thurau: Establishment of SSH library, selection of candidate genes, gene expression analysis. Lisa Krapoth: Arabidopsis mutant phenotyping. Andrea Schuster: TILLING mutant phenotyping. Zheng Zhou/Wanzhi Ye: gene expression analysis. Steffen Rietz/Gunhild Leckband: Project industry partner, responsible for plant transformation and seed propagation. Daguang Cai: Project strategies and experimental design, finalizing the manuscript.

## References

Acevedo-Garcia, J., Spencer, D., Thieron, H., Reinstädler, A., Hammond-Kosack, K., Phillips, A.L. and Panstruga, R. (2017) mlo-based powdery mildew resistance in hexaploid bread wheat generated by a non-transgenic TILLING approach. *Plant Biotechnol. J.* **15**, 367–378.

Altschul, S.F., Gish, W., Miller, W., Myers, E.W. and Lipman, D.J. (1990) Basic local alignment search tool. *J. Mol. Biol.* **215**, 403–410.

 

Bae, S., Park, J. and Kim, J.S. (2014) Cas-OFFinder: a fast and versatile algorithm that searches for potential off-target sites of Cas9 RNA-guided endonucleases. *Bioinformatics*, **30**, 1473–1475.

Behrens, F.H., Schenke, D., Hossain, R., Häder, C., Zhao, Y., Zhu, W. and Cai, D. (2019) Suppression of abscisic acid (ABA) biosynthesis at the early infection stage of *Verticillium longisporum* in oilseed rape (*Brassica napus*). *Mol. Plant Pathol.* **20**,1645–1661.

Berardini, T.Z., Reiser, L., Li, D., Mezheritsky, Y., Muller, R., Strait, E. and Huala, E. (2015) The Arabidopsis information resource: making and mining the "gold standard" annotated reference plant genome. *Genesis*, **53**, 474–85.

Blom, N., Sicheritz-Ponten, T., Gupta, R., Gammeltoft, S. and Brunak, S. (2004) Prediction of post-translational glycosylation and phosphorylation of proteins from the amino acid sequence. *Proteomics*, **4**, 1633–1649.

Braatz, J., Harloff, H.J., Mascher, M., Stein, N., Himmelbach, A. and Jung, C. (2017) CRISPR-Cas9 targeted mutagenesis leads to simultaneous modification of different homoeologous gene copies in polyploid oilseed rape (*Brassica napus*). *Plant Physiol.* **174**, 935–942.

Campbell, C.L. and Madden, L.V. (1990) *Introduction to plant disease epidemiology*. New York: Wiley. http://www.loc.gov/catdir/enhancements/fy0706/89034349-b.html.

Chalhoub, B., Denoeud, F., Liu, S., Parkin, I.A.P., Tang, H. *et al*. (2014) Early allopolyploid evolution in the post-Neolithic *Brassica napus* oilseed genome. *Science*, **354**, 950–953.

Chandrasekaran, J., Brumin, M., Wolf, D., Leibman, D., Klap, C., Pearlsman, M., Sherman, A. *et al*. (2016) Development of broad virus resistance in non-transgenic cucumber using CRISPR/Cas9 technology. *Mol. Plant Pathol.* **17**, 1140–1153.

Chen, M.-H., Tian, G.-W., Gafni, Y. and Citovsky, V. (2005) Effects of Calreticulin on viral cell-to-cell movement. *Plant Physiol.* **138**, 1866–1876.

Chen, Y.F., Shakeel, S.N., Bowers, J., Zhao, X.C., Etheridge, N. and Schaller, G.E. (2007) Ligand-induced degradation of the ethylene receptor ETR2 through a proteasome-dependent pathway in Arabidopsis. *J. Biol. Chem.* **282**, 24752–8.

Christensen, A., Svensson, K., Persson, S., Jung, J., Michalak, M., Widell, S. and Sommarin, M. (2008) Functional characterization of Arabidopsis Calreticulin1a: a key alleviator of endoplasmic reticulum stress. *Plant Cell Physiol.* **49**, 912–924.

Christensen, A., Svensson, K., Thelin, L., Zhang, W., Tintor, N., Prins, D., Funke, N. *et al*. (2010) Higher plant Calreticulins have acquired specialized functions in Arabidopsis. *PLoS ONE*, **5**, 1–18.

Coppolino, M.G. and Dedhar, S. (1998) Molecules in focus: calreticulin. *Int. J. Biochem. Cell Biol.* **30**, 553–558.

Cohn, M., Bart, R.S., Shybut, M., Dahlbeck, D., Gomez, M., Morbitzer, R., Hou, B.H. *et al*. (2014) Xanthomonas axonopodis virulence is promoted by a transcription activator-like effector-mediated induction of a SWEET sugar transporter in cassava. *Mol. Plant Microbe Interact.* **27**, 1186–98.

Depotter, J.R., Deketelaere, S., Inderbitzin, P., von Tiedemann, A., Höfte, M., Subbarao, K.V., Wood, T.A. *et al*. (2016) *Verticillium longisporum*, the invisible threat to oilseed rape and other Brassicaceous plant hosts. *Mol. Plant Pathol.* **17**, 1004–1016.

De Coninck, B., Timmermans, P., Vos, C., Cammue, B.P.A. and Kemal, K. (2015) What lies beneath: belowground defense strategies in plants. *Trends Plant Sci.* **20**, 91–101.

Diatchenko, L., Lau, Y.-F.C., Campbell, A.P., Chenchik, A., Moqadam, F., Huang, B., Lukyanov, S. *et al*. (1996) Suppression subtractive hybridization: a method for generating differentially regulated or tissue-specific cDNA probes and libraries. *Proc. Natl. Acad. Sci. USA*, **93**, 6025–6030.

Danilczyk, U.G., Cohen-Doyle, M.F. and Williams, D.B. (2000) Functional relationship between Calreticulin, Calnexin, and the endoplasmic reticulum luminal domain of Calnexin. *J. Biol. Chem.* **275**, 13089–13097.

Das, S., Dutta, S.S., Chowdhury, S. and Das, K. (2015) Ethylene signal transduction and signaling roles – a review. *Agri. Rev.* **36**, 133–139.

Denecke, J., Carlsson, L.E., Vidal, S., Höglund, A.-S., Ek, B., van Zeijl, M.J., Sinjorgo, K.M.C. *et al*. (1995) The tobacco homolog of mammalian Calreticulin is present in protein complexes *in vivo*. *Plant Cell*, **7**, 391–406.

Dunker, S., Keunecke, H., Steinbach, P. and von Tiedemann, A. (2008) Impact of *Verticillium longisporum* on yield and morphology of winter oilseed rape (*Brassica napus*) in relation to systemic spread in the plant. *J. Phytopathol.* **156**, 698–707.

Eynck, C., Koopmann, B., Grunewald-Stoecker, G., Karlovsky, P. and von Tiedemann, A. (2007) Differential interactions of *Verticillium longisporum* and *V. dahliae* with *Brassica napus* detected with molecular and histological techniques. *Eur. J. Plant Pathol.* **118**, 259–274.

Eynck, C., Koopmann, B., Karlovsky, P. and von Tiedemann, A. (2009) Internal resistance in winter oilseed rape inhibits systemic spread of the vascular pathogen *Verticillium longisporum*. *Phytopathology*, **99**, 802–811.

FAOSTAT. (2016) *Statistical database. Food and Agriculture Organization of the United Nations: Statistic Division*. Available at: http://www.fao.org/faostat/en/#data/QC/visualize. Accessed: 09/12/2016.

Fröschel, C., Iven, T., Walper, E., Bachmann, V., Weiste, C. and Dröge-Laser, W. (2019) A gain-of-function screen reveals redundant ERF transcription factors providing opportunities for resistance breeding toward the vascular fungal pathogen *Verticillium longisporum*. *Mol. Plant Microbe Interact.* **32**, 1095–1109.

Gallie, D.R. (2015) Ethylene receptors in plants – why so much complexity? *F1000Prime Rep.* **7**, 39.

Garg, G., Yadav, S. and Ruchi, Y.G. (2015) Key roles of Calreticulin and Calnexin proteins in plant perception under stress conditions: a review. *Adv. Life Sci.* **5**, 18–26.

Happstadius, I., Ljungberg, A., Kristiansson, B. and Dixelius, C. (2003) Identification of *Brassica oleracea* germplasm with improved resistance to Verticillium wilt. *Plant Breed.* **122**, 30–34.

Harloff, H.-J., Lemcke, S., Mittasch, J., Frolov, A., Wu, J.G., Dreyer, F., Leckband, G. *et al*. (2012) A mutation screening platform for rapeseed (*Brassica napus* L.) and the detection of sinapine biosynthesis mutants. *Theor. Appl. Genet.* **124**, 957–969.

Hatzig, S., Breuer, F., Nesi, N., Ducournau, S., Wagner, M.H., Leckband, G., Abbadi, A. *et al*. (2018) Hidden effects of seed quality breeding on germination in oilseed rape (*Brassica napus* L.). *Front. Plant Sci.* **9**, 419.

Henikoff, S., Till, B.J. and Comai, L. (2004) TILLING. Traditional mutagenesis meets functional genomics. *Plant Physiol.* **135**, 630–636.

Hruz, T., Laule, O., Szabo, G., Wessendorp, F., Bleuler, S., Oertle, L., Widmayer, P. *et al*. (2008) Genevestigator v3: a reference expression database for the meta-analysis of transcriptomes. *Adv. Bioinformatics*, 420747. https://doi.org/10.1155/2008/420747.

Hu, Y., Zhang, J., Jia, H., Sosso, D., Li, T., Frommer, W.B., Yang, B. *et al*. (2014) Lateral organ boundaries 1 is a disease susceptibility gene for citrus bacterial canker disease. *Proc. Natl. Acad. Sci. USA*, **111**, E521–E529.

Johansson, A., Staal, J. and Dixelius, C. (2006) Early responses in the *Arabidopsis-Verticillium longisporum* pathosystem are dependent on *NDR1*, JA- and ET-associated signals via cytosolic NPR1 and *RFO1*. *Mol. Plant Microbe Interact.* **19**, 958–969.

Joshi, R., Paul, M., Kumar, A. and Pandey, D. (2019) Role of calreticulin in biotic and abiotic stress signalling and tolerance mechanisms in plants. *Gene*, **714**, 144004.

Jia, X.-J., He, L.-H., Jing, R.-L. and Li, R.-Z. (2009) Calreticulin: conserved protein and diverse functions in plants. *Physiol. Plant.* **136**, 127–138.

Ju, C. and Chang, C. (2015) Mechanistic insights in ethylene perception and signal transduction. *Plant Physiol.* **169**, 85–95.

Kallimasioti-Pazi, E.M., Thelakkad, C.K., Taylor, G.C., Meynert, A., Ballinger, T., Kelder, M.J.E., Lalevée, S. *et al*. (2018) Heterochromatin delays CRISPR-Cas9 mutagenesis but does not influence the outcome of mutagenic DNA repair. *PLoS Biol.* **16**, e2005595.

Kang, H.-G., Oh, C.-S., Sato, M., Katagiri, F., Glazebrook, J.-, Takahashi, H. *et al*. (2010) Endosome-associated CRT1 functions early in resistance gene-mediated defense signaling in Arabidopsis and tobacco. *Plant Cell*, **22**, 918–936.

Kim, J.H., Nguyen, N.H., Nguyen, N.T., Hong, S.-H. and Lee, H. (2013) Loss of all three calreticulins, CRT1, CRT2 and CRT3, causes enhanced sensitivity to water stress in Arabidopsis. *Plant Cell Rep.* **32**, 1843–1853.

Krause, K.-H. and Michalak, M. (1997) Calreticulin. *Cell*, **88**, 439–443.

Kusch, S. and Panstruga, R. (2017) mlo-based resistance: an apparently universal "weapon" to defeat powdery mildew disease. *Mol. Plant Microbe Interact.* **30**, 179–189.

Langner, T., Kamoun, S. and Belhaj, K. (2018) CRISPR Crops: plant genome editing toward disease resistance. *Annu. Rev. Phytopathol.* **56**, 479–512.

Li, J., Zhao-Hui, C., Batoux, M., Nekrasov, V., Roux, M., Chinchilla, D., Zipfel, C. *et al*. (2009) Specific ER quality control components required for biogenesis of the plant innate immune receptor EFR. *Proc. Natl. Acad. Sci. USA*, **106**, 15973–15978.

Li, J.F., Norville, J.E., Aach, J., McCormack, M., Zhang, D., Bush, J., Church, G.M. *et al*. (2013) Multiplex and homologous recombination-mediated genome editing in *Arabidopsis* and *Nicotiana benthamiana* using guide RNA and Cas9. *Nat. Biotechnol.* **31**, 688–691.

Liebrand, T.W.H., Kombrink, A., Zhang, Z., Sklenar, J., Jones, A.M.E., Robatzek, S., Thomma, B.P.H.J. *et al*. (2014) Chaperones of the endoplasmic reticulum are required for Ve1-mediated resistance to *Verticillium*. *Mol. Plant Pathol.* **15**, 109–117.

Macovei, A., Sevilla, N.R., Cantos, C., Jonson, G.B., Slamet-Loedin, I., Cermak, T., Voytas, D.F. *et al*. (2018) Novel alleles of rice eIF4G generated by CRISPR/Cas9-targeted mutagenesis confer resistance to rice tungro spherical virus. *Plant Biotechnol. J.* **16**, 1918–1927.

Malnoy, M., Viola, R., Jung, M.-H., Koo, O.-J., Kim, S., Kim, J.-S., Velasco, R. *et al*. (2016) DNA-free genetically edited grapevine and apple protoplast using CRISPR/Cas9 ribonucleoproteins. *Front. Plant Sci.* **7**, 1904.

McCallum, C.M., Comai, L., Greene, E.A. and Henikoff, S. (2000) Targeting Induced Local Lesions IN Genomes (TILLING) for plant functional genomics. *Plant Physiol.* **123**, 439–442.

Menegazzi, P., Guzzo, F., Baldan, B., Mariani, P. and Treves, S. (1993) Purification of Calreticulin-like protein(s) from spinach leaves. *Biochem. Biophys. Res. Comm.* **190**, 1130–1135.

Merchante, C., Alonso, J.M. and Stepanova, A.N. (2013) Ethylene signaling: simple ligand, complex regulation. *Curr. Opin. Plant Biol.* **16**, 554–560.

Mikami, M., Toki, S. and Endo, M. (2015) Parameters affecting frequency of CRISPR/Cas9 mediated targeted mutagenesis in rice. *Plant Cell Rep.* **34**, 1807–1815.

Nagaharu, U. (1935) Genome analysis in Brassica with special reference to the experimental formation of B. napus and peculiar mode of fertilization. *Japan. J. Bot.* **7**, 389–452.

Nakagawa, T., Suzuki, T., Murata, S., Nakamura, S., Hino, T., Maeo, K., Tabata, R. *et al*. (2007) Improved Gateway binary vectors: high-performance vectors for creation of fusion constructs in transgenic analysis of plants. *Biosci. Biotechnol. Biochem.* **71**, 2095–2100.

Neff, M.M., Neff, J.D., Chory, J. and Pepper, A.E. (1998) dCAPS, a simple technique for the genetic analysis of single nucleotide polymorphisms: experimental applications in Arabidopsis thaliana genetics. *Plant J.* **14**, 387–92.

Nekrasov, V., Wang, C., Win, J., Lanz, C., Weigel, D. and Kamoun, S. (2017) Rapid generation of a transgene-free powdery mildew resistant tomato by genome deletion. *Sci. Rep.* **7**, 482.

Okubara, P.A. and Paulitz, T.C. (2005) Root defense responses to fungal pathogens: a molecular perspective. *Plant Soil.* **274**, 215–226.

Oliva, R., Ji, C., Atienza-Grande, G., Huguet-Tapia, J.C., Perez-Quintero, A., Li, T., Eom, J.-S. *et al*. (2019) Broad-spectrum resistance to bacterial blight in rice using genome editing. *Nat. Biotechnol.* **37**, 1344–1350.

Okuzaki, A., Ogawa, T., Koizuka, C., Kaneko, K., Inaba, M., Imamura, J. and Koizuka, N. (2018) CRISPR/Cas9-mediated genome editing of the fatty acid desaturase 2 gene in Brassica napus. *Plant Physiol Biochem.* **131**, 63–69. https://doi.org/10.1016/j.plaphy.2018.04.025

Ostwald, T.J. and MacLennan, D.H. (1974) Isolation of a high affinity calcium-binding protein from sarcoplasmic reticulum. *J. Biol. Chem.* **249**, 974–979.

Pantelides, I.S., Tjamos, S.E. and Paplomatas, E.J. (2010) Ethylene perception via ETR1 is required in Arabidopsis infection by Verticillium dahliae. *Mol Plant Pathol.* **11**(2), 191–202.

Park, J., Bae, S. and Kim, J.S. (2015) Cas-Designer: a web-based tool for choice of CRISPR-Cas9 target sites. *Bioinformatics*, **31**, 4014–4016.

Reusche, M., Thole, K., Janz, D., Truskina, J., Rindfleisch, S., Drübert, C., Polle, A. *et al*. (2012) *Verticillium* infection triggers VASCULAR-RELATED NAC DOMAIN7-dependent de novo xylem formation and enhances drought tolerance in *Arabidopsis*. *Plant Cell*, **24**, 3823–3837.

Rogers, S.O. and Bendich, A.J. (1985) Extraction of DNA from milligram amounts of fresh, herbarium and mummified plant tissues. *Plant Mol. Biol.* **5**, 69–76.

Rygulla, W., Snowden, R.J., Friedt, W., Happstadius, I., Cheung, W.Y. and Chen, D. (2008) Identification of quantitative trait loci for resistance against *Verticillium longisporum* in oilseed rape (*Brassica napus*). *Phytopathology*, **98**, 215–221.

Sarwat, M. and Tuteja, N. (2017) How the ER Stress Protein Calreticulins Differ from Each Other in Plants?. In *Plant Bioinformatics*, pp. 403–415. Cham: Springer. https://doi.org/10.1007/978-3-319-67156-7_17

Schiml, S., Fauser, F. and Puchta, H. (2014) The CRISPR/Cas system can be used as nuclease for in planta gene targeting and as paired nickases for directed mutagenesis in Arabidopsis resulting in heritable progeny. *Plant J.* **80**, 1139–50.

Shakeel, S.N., Gao, Z., Amir, M., Chen, Y.F., Rai, M.I., Haq, N.U. and Schaller, G.E. (2015) Ethylene regulates levels of ethylene receptor/CTR1 signaling complexes in *Arabidopsis thaliana*. *J. Biol. Chem.* **290**, 12415–12424.

Stein, N., Perovic, D., Kumlehn, J., Pellio, B., Stracke, S., Streng, S., Ordon, F. *et al*. (2005) The eukaryotic translation initiation factor 4E confers multiallelic recessive Bymovirus resistance in *Hordeum vulgare* (L.). *Plant J.* **42**, 912–22.

Sun, Q., Lin, L., Liu, D., Wu, D., Fang, Y., Wu, J. and Wang, Y. (2018) CRISPR/Cas9-mediated multiplex genome editing of the BnWRKY11 and BnWRKY70 genes in *Brassica napus* L. *Int. J. Mol. Sci.* **19**(9), pii: E2716. https://doi.org/10.3390/ijms19092716

Tamura, K., Stecher, G., Peterson, D., Filipski, A. and Kumar, S. (2013) MEGA6: molecular evolutionary genetics analysis version 6.0. *Mol. Biol. Evol.* **30**, 2725–2729.

Till, B.J., Zerr, T., Comai, L. and Henikoff, S. (2006) A protocol for TILLING and Ecotilling in plants and animals. *Nat. Protoc.* **5**, 2465–2477.

Tsolakidou, M.D., Pantelides, I., Tzima, A.K., Kang, S., Paplomatas, E.J. and Tsaltas, D. (2019) Disruption and overexpression of the gene encoding ACC (1-Aminocyclopropane-1-Carboxylic Acid) deaminase in soil-borne fungal pathogen *Verticillium dahliae* revealed the role of ACC as a potential regulator of virulence and plant defense. *Mol. Plant Microbe Interact.* **32**, 639–653.

Urnov, F.D., Ronald, P.C. and Carroll, D. (2018) A call for science-based review of the European court's decision on gene-edited crops. *Nat. Biotechnol.* **36**, 800–802.

USDA: Crop Production. (2018) *Summary*. February 2019. ISSN: 1057-7823.

Verkuijl, S.A. and Rots, M.G. (2019) The influence of eukaryotic chromatin state on CRISPR-Cas9 editing efficiencies. *Curr. Opin. Biotechnol.* **55**, 68–73.

Wang, Y., Cheng, X., Shan, Q., Zhang, Y., Liu, J., Gao, C. and Qiu, J.-L. (2014) Simultaneous editing of three homoeoalleles in hexaploid bread wheat confers heritable resistance to powdery mildew. *Nat. Biotechnol.* **32**, 947–951.

Wilson, R.L., Kim, H., Bakshi, A. and Binder, B.M. (2014) The ethylene receptors ETHYLENE RESPONSE1 and ETHYLENE RESPONSE2 have contrasting roles in seed germination of Arabidopsis during salt stress. *Plant Physiol.* **165**, 1353–1366.

Xiong, X., Sun, S., Zhang, X., Li, Y., Liu, F., Zhu, Q., Xeu, F. *et al*. (2020) GhWRKY70D13 regulates resistance to *Verticillium dahliae* in cotton through the ethylene and jasmonic acid signaling pathways. *Front. Plant Sci.*, **11**, 69. https://doi.org/10.3389/fpls.2020.00069.

Yang, H., Wu, J.J., Tang, T., Liu, K.D. and Dai, C. (2017) CRISPR/Cas9-mediated genome editing efficiently creates specific mutations at multiple loci using one sgRNA in *Brassica napus*. *Sci. Rep.* **7**, 7489.

Yang, Y., Zhu, K., Li, H., Han, S., Meng, Q., Khan, S.U., Fan, C. *et al*. (2018) Precise editing of CLAVATA genes in *Brassica napus* L. regulates multilocular silique development. *Plant Biotechnol. J.* **16**, 1322–1335.

Zeise, K. and von Tiedemann, A. (2002) Host specialization among vegetative compatibility groups of *Verticillium dahliae* in relation to *Verticillium longisporum*. *J. Phytopathol.* **150**, 112–119.

Zhai, Y., Cai, S., Hu, L., Yang, Y., Amoo, O., Fan, C. and Zhou, Y. (2019a) CRISPR/Cas9-mediated genome editing reveals differences in the contribution of INDEHISCENT homologues to pod shatter resistance in *Brassica napus* L. *Theor. Appl. Genet.* **132**, 2111–2123.

Zhai, Y., Yu, K., Cai, S., Hu, L., Amoo, O., Xu, L., Yang, Y. *et al*. (2019b) Targeted mutagenesis of BnTT8 homologs controls yellow seed coat development for effective oil production in *Brassica napus* L. *Plant Biotechnol. J.* **18**, 1153–1168.

Zhao, J. and Meng, J. (2003) Detection of loci controlling seed glucosinolate content and their association with *Sclerotinia* resistance in *Brassica napus*. *Plant Breed.* **122**, 19–23.

Zheng, M., Zhang, L., Tang, M., Liu, J., Liu, H., Yang, H., Fan, S. *et al*. (2019) Knockout of two BnaMAX1 homologs by CRISPR/Cas9-targeted mutagenesis

improves plant architecture and increases yield in rapeseed (*Brassica napus* L.). *Plant Biotechnol. J.* **18**, 644–654.

Zhou, J., Peng, Z., Long, J., Yang, B. (2015) Gene targeting by the TAL effector PthXo2 reveals cryptic resistance gene for bacterial blight of rice. *Plant J.* **82**, 632–643.

## Supporting information

Additional supporting information may be found online in the Supporting Information section at the end of the article.

**Figure S1** Verification of the SSH libraries.
**Figure S2** Time course of infection with *Vl43* and determination of optimal conidia concentration.
**Figure S3** There are 4 *CRT1a* loci in the *Brassica napus* genome.
**Figure S4** The SSH-EST 6F11-F8 corresponds to BnaA09g15400D (SNPs highlighted in red).
**Figure S5** Flow chart for CRISPR/Cas vector construction.
**Figure S6** dCAPS-analysis of positive CRISPR events.
**Figure S7** Effect of *CRT1a* mutations on 1000 seed weight.
**Figure S8** Phenotype of C4E23 at 28 dpi with *Verticillium longisporum* using $1 \times 10^7$ spores/mL.
**Figure S9** Detection of transgene-free plants.
**Figure S10** Analysis of CRT1a on amino acid level.
**Table S1** SSH library (EXCEL).
**Table S2** Genevestigator Meta-Analysis of SSH candidate genes (EXCEL).
**Table S3** Candidate genes selected from the SSH libraries.
**Table S4** Agronomic traits investigated under control and infection conditions.
**Table S5** TILLING statistics of *CRT1a* screen within an EMS mutagenized population.
**Table S6** Primer-Information (EXCEL).
**Table S7** Disease rating scale for Verticillium infection of Brassica napus plants (Enyck *et al.* 2007).